HYDROCOASTAL

SAR/SARin Radar Altimetry for Coastal Zone and Inland Water Level

Coastal and FF-SAR processing of S6 data
Technical Note, CCN#2, deliverable D2

Sentinel-3 and Cryosat SAR/SARin Radar Altimetry for Coastal Zone and Inland Water

ESA Contract 4000129872/20/I-DT

Project reference: HYDROCOASTAL_ESA_TN_CCN2_D2
Issue: 1.0

This page has been intentionally left blank

Change Record

Date	Issue	Section	Page	Comment
25/07/2023	1.0	all	all	1st version

Control Document

Process	Name	Date
Written by:	Pablo García, Ferran Gibert, Alba Granados	25/07/2023
Checked by	David Cotton	
Approved by:		

Subject	Radar Altimetry for Coastal Zone and Inland Water Level	Project	HYDROCOASTAL
Author	Organisation	Internal references	
Pablo García, Ferran Gibert, Alba Granados	isardSAT	HYDROCOASTAL_ESA_TN_CCN2_D1	
	Along Track		
	Aresys		
	DTU Space		
	TUM		
	U Bonn		

	Signature	Date
For HYDROCOASTAL team		
For ESA		

Table of Contents

1. Introduction

1.1. The HYDROCOASTAL Project

The HYDROCOASTAL project is a project funded under the ESA EO Science for Society Programme and aims to maximise the exploitation of SAR and SARin altimeter measurements in the coastal zone and inland waters, by evaluating and implementing new approaches to process SAR and SARin data from CryoSat-2, and SAR altimeter data from Sentinel-3A and Sentinel-3B.

One of the key objectives is to link together and better understand the interactions processes between river discharge and coastal sea level. Key outputs are global coastal zone and river discharge data sets, and assessments of these products in terms of their scientific impact.

1.2. Scope of this Document

This is the Technical Note corresponding to the CCN 2 of the project and represents the deliverable D2 of the CCN.

The purpose of this document is to describe the work carried out covering two different studies using Sentinel-6 data. So far in the project, only Sentinel-3A/B products have been considered.

The first study is focused on the coastal processing using the CORS (Coastal Ocean Retracker for the Sentinels) processor and in the later assessment of the results obtained. The areas of study are coincident with the already considered during the project: the Baltic Sea, the California coast, and the Aegean Sea.

The second study corresponds to the use of the FF-SAR isardSAT processor over one specific track of interest on the coasts of the Aegean Sea islands. The combination of the CORS processor techniques with the FF-SAR processing, initially not considered in the scope of the CCN, is an added effort that has been made finally possible. The benefits of the increased spatial resolution, altogether with the coastal specialized algorithms, are analysed producing different metrics.

1.3. Applicable Documents

AD-01: Sentinel-3 and CryoSat SAR/SARin Radar Altimetry for COASTAL ZONE and INLAND WATER - Statement of Work, V1.0 10/01/2019 Ref: EOP-SD-SOW-2018-089

1.4. Reference Documents

RD-01 HYDROCOASTAL Technical Proposal. V1.1 28/11/2019, SatOC and HYDROCOASTAL team.
RD-02 HYDROCOASTAL Implementation Proposal. V1.1 28/11/2019, SatOC and HYDROCOASTAL team.
RD-03 HYDROCOASTAL Management Proposal. V1.3 26/11/2019, SatOC and HYDROCOASTAL team
RD-04 HYDROCOASTAL Financial Proposal. V1.2 28/11/2019, SatOC and HYDROCOASTAL team

RD-05 HYDROCOASTAL Contractual Proposal. V 1.2 26/11/2019, SatOC and HYDROCOASTAL team
RD-06 HYDROCOASTAL Deliverable 1.3 ATBD (Algorithm Theoretical Basis Document). V1.1 08/10/2020, isardSAT and HYDROCOASTAL team.
RD-07 HYDROCOASTAL POCCD (Processing Option Configuration Control Document). V1.1 08/10/2020, isardSAT and HYDROCOASTAL team.
RD-08 HYDROCOASTAL Deliverable 2.1 IODD (Input Output Data Definitions). V1.1 08/10/2020, isardSAT and HYDROCOASTAL team.
RD-09 HYDROCOASTAL Deliverable 2.3 PSD (Product Specification Document). V1.1 08/10/2020, isardSAT and HYDROCOASTAL team.

1.5. Document Organisation

After this introductory section, section 2 covers the study of the CORS processor outputs, explaining the inputs and areas considered, the processing specifics and its outputs and finally the analysis of the results. Section 3 follow the same structure of section 2 but regarding the FF-SAR study processing and assessment.

2. Sentinel-6 Coastal Processor (CORS) exploitation and assessment

This section describes the inputs and algorithms used for the DD coastal processing, and the assessment of the results from its run. One year of Sentinel-6 data have been considered for the study. The approach of the CORS coastal processor is the same explained in the recent Living Planet Symposium 2022 symposium, the S6VT meetings (https://cdn.eventsforce.net/files/ef-xnn67yq56ylu/website/26/2.2_garcia-_isardsat_corals_s6vt_2_20210520.pdf), and the OSTST (https://ostst.aviso.altimetry.fr/fileadmin/user_upload/OSTST2022/Presentations/COA2022-Coastal_Processing_from_the_Copernicus_Altimeters__the_CORS_processor_outcomes.pdf).

2.1. Input Data and Areas of Interest

For the DD Coastal Processing study, we have decided to choose the same areas considered in previous stages of this project, for the sake of comparison, although the missions are not coincident.

These areas are:

- Aegean Sea
- Baltic Sea
- California Coast

The three areas represent differentiated sea state conditions and coastal topography casuistic, hence it is a good candidate for the study of coastal altimetry algorithms. The areas are represented in Figure 1.

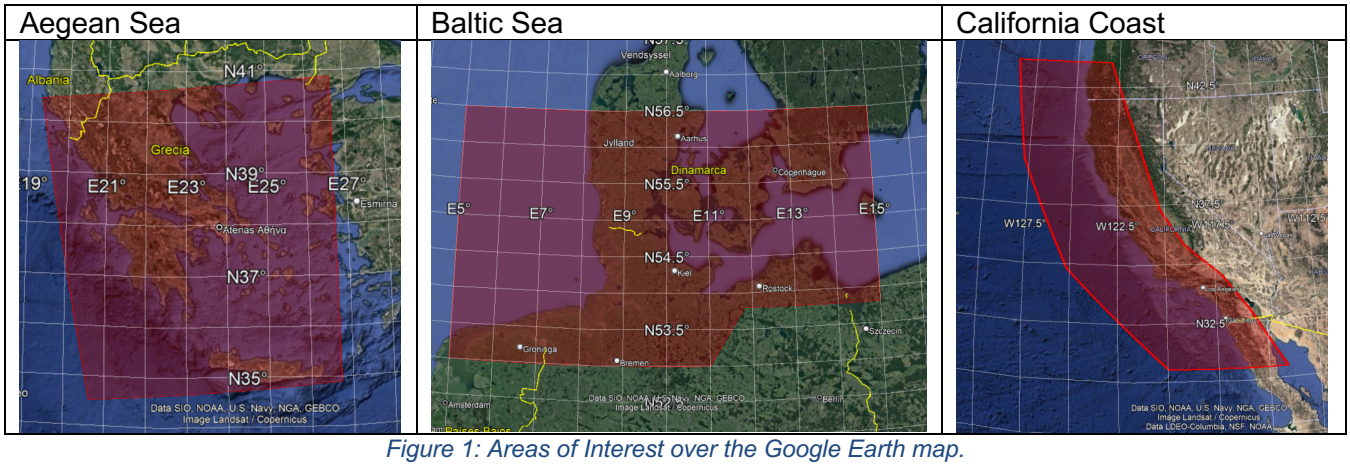

Figure 1: Areas of Interest over the Google Earth map.

L1B NTC and L2 NTC data have been downloaded from the EUMETSAT EO Portal. The number of products for each area is shown in . The data used corresponds to reprocessed F06 data. Hence, we have a homogeneous updated dataset. The cycles included are from cycle 5 to cycle 42.

Table 1: Size of each Area of Interest dataset.

	Aegean Sea	Baltic Sea	California Coast
Number of products	209	279	245

For the statistical analysis of the coastal altimetry data, a limit of 30 km to the coast was considered. Nevertheless, for some specific metrics, tighter boundaries have been set (e.g. analysis of the strict set of distances to the coast impacted by the land contamination). Figure 2 shows the tracks sections up to 30 km from the coast of each area of interest dataset.

Aegean Sea	Baltic Sea	California Coast
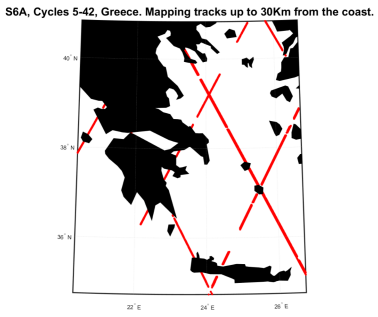	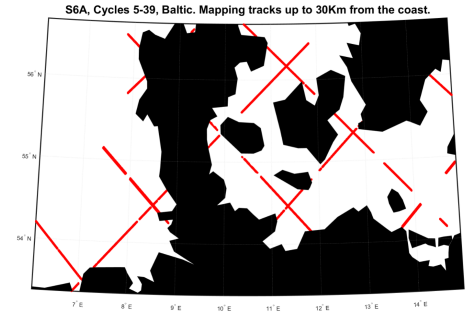	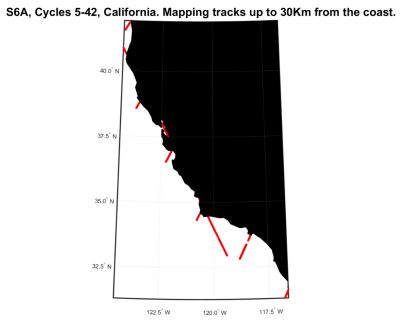

Figure 2: Tracks sections of maximum 30 km from the coast considered in the study

2.2. Processing and results

The CORS processor algorithms are the result of different stages of development from an original idea of a CryoSat-2 coastal processor within the scope of the CP4O (CryoSat Plus for Oceans) ESA project. The core concept has not changed: we try to avoid the maximum number of interferences of the science waveform by cutting and retracking a section of it.

For doing so we must define a reference within the window that coincides with the expected location of the ocean surface height. In addition, we set a number of samples to consider for the retracking on the left and on the right of the defined reference.

The reference can be defined from different approaches. The CP4O initial idea, as explained in (García, et al. 2018), consisted in a combination of thresholds within the 3 SARin waveforms: Coherence, Phase Difference and Power. Thresholds of high coherence, low phase difference (angle of arrival) and high power, are consecutively set in order to give a final reference around Nadir Ocean. The drawback of this solution was that only SAR interferometry mode, so far available only for the CryoSat-2 mission, could be processed. It is the only mode offering the information of the angle of arrival across-track.

Consequently, a window reference solution usable for all altimetry missions was investigated. A window delay (tracker range) approach was adopted. The assumption that the sea surface elevations are not expected to vary considerably (covering one nominal range bin) between consecutive records along track (300 m) induced the idea of a stable tracker range elevation. Any jump of the tracker range would be then used to compensate for it and define the window reference for the waveform cut. This is valid for a closed loop tracking scenario and is the second option shown in (García, et al. 2018).

But now it is more and more common to see altimetry missions, like the Copernicus constellation ones, exploiting the open loop tracking mode. In this case a DEM is the responsible of the tracking window positioning. It forces a redefinition of the coastal processor algorithm because the jumps of the tracker range over the ocean could be no longer due to an off-nadir bright target tracking but caused by the DEM onboard instruction itself.

This leads to the current approach. The reference positioning will be defined now from an external model. The Geoid or the Mean Sea Surface (MSS) are candidates for setting the specific range bin to cut the waveform around. The Geoid option was dropped in favour of the MSS one, after an analysis. It was clear that the MSS was showing much more detail and realistic ocean surface elevation, when comparing to Open Ocean retracking results, which tend to be stable. As in previous approaches, here we preserve the use of available data, without the need of external sources of information or models. The MSS data series is available at L2 products; hence we can extract this field from the corresponding L2 file.

Once solved the range reference, we need to establish a window width for the generation of the sub-waveform. After a test bench assessment combining different left and right number of samples, it was decided that the optimum setting for Sentinel-3 missions was: 15 left range bins and 5 right range bins. The number of left range bins shall cover the whole leading edge of the waveform and enough samples for a correct estimation of the thermal noise. The number of right range bins are the minimum necessary to perform the retracker fitting, avoiding the maximum number of interferences located in the trailing edge without compromising the goodness of fit.

All the above algorithms explained corresponds to what we call post-L1B stage of the CORS processor. A second (and final) stage is the retracking of the sub-waveform.

The CORS retracking stage is based on the SAR ocean analytical model described in (Ray *et al.*, 2015) and shaped to the characteristics of the L1B processor (Makhoul *et al.*, 2018). Several modifications have been carried out to cope with a sub-waveform retracking, and to the different missions in the last years, the last being Sentinel-6. The thermal noise estimation method has been modified for the case of altimetric echoes from coastal regions. Since strong off-nadir reflections might occur due to land contamination, an alternative to a fixed window strategy for the thermal noise computation is considered, consisting of a dynamic window limited by the automatically detected toe of the leading edge and a possible off-nadir reflection previous in time. In addition, the selection of the initial geophysical parameters estimates has been optimised to improve the fitting procedure. The selection of these estimates has been shown to have an effect on the final retracked time series, such as divergence issues or spurious energy distribution of some parameters. A specific strategy has been followed to overcome these limitations, consisting of the application of a moving window to previous estimates to obtain initial estimates at a current surface.

The application of this solution was carried out for the Sentinel-6 Validation Team initiative for a limited dataset. Now, these three Hydrocoastal project areas of interest will enlarge the variety of validation scenarios of the CORS coastal processor solution.

2.2.1. The distance to the coast solution.

Before explaining the assessment of the results, we want to mention a crucial element in the validation of the results. For the development of the different diagnosis of the geophysical retrievals in the coastal Ocean scenario, the distance to the coast (d2c) is a key element. When analysing the results, it is especially interesting in this context to evaluate the different outcomes in relation to the distance to the closest land point.

The official L2 product contains information of this parameter, which is computed from a GSHHS solution. We have observed that the lack of accuracy of the d2c L2 field causes a general inconsistence in the analysis of the results, making it difficult to extract sound conclusions when this parameter is involved.

isardSAT has developed a d2c solution with a much higher resolution and an almost exact match with the georeferenced maps. This solution is based on a processing of the coastline polylines included in a collaborative open-source platform: the Open Street Map (OSM). Coastline polygons are closed forming a global database. This database can be easily scalable to a specific area of study, in order to reduce the computational effort when retrieving the d2c from every science product record to the closest OSM polygon.

The comparisons between the isardSAT and the official L2 products using this OSM d2c parameter are notably more coherent than making use of the L2 product d2c field. This is of great help in understanding and extracting conclusions in the analysis versus d2c.

2.2.2. Analysis of the estimated geophysical parameters noise.

The three geophysical parameters below have been analysed in this validation exercise:

- Sea Surface Height (SSH)
- Significant Wave Height (SWH)
- Sigma0 (used mainly for the winds retrievals)

The level of noise of the 3 geophysical estimations is analysed in this chapter.

Two kinds of representation are considered for showing the performances in terms of stability.

The first representation is the parameter noise as a function of the distance to the coast. Typically, the noise tends to increase at around 8 km from the coast, where the tracking window starts to show the impact of interferences of coastal environments. These interferences are originated usually by land bright targets or specular coastal waters. Some of them are brighter enough to cause the retracker to follow them along their parabolic travel within the radargram section of several consecutive records.

The figure of the noise vs distance to the coast gives us a qualitative idea of how much CORS can get close to the coast without increasing a parameter noise level over a threshold.

A quantitative value for this validation is the noise improvement ratio of CORS with respect to the EUMETSAT products of each of the 3 estimations.

Usually, the SSH ratio improvement is the highest of the three, for this coastal algorithm being designed initially specifically for the SSH parameter.

The second representation is the histogram of the differences along track of a parameter. These differences are expected to be small over the ocean. Any wrong estimation of a parameter will increase the difference between records, and therefore it will be represented in the figure far from the zero value. For instance, for the SSH estimation, an ideal histogram is a narrow figure tending to the value of the along track mean sea slope of the studied area. Wider figures will show worse stability.

Here below we will show the first of the two kinds of figures: the noise level as a function of the distance to the coast.

In each page we will represent the three parameters (i.e., SSH, SWH & Sigma0) for a specific area of interest: Greece (Figure 3), Baltic (Figure 4) and California (Figure 5).

The quantitative results for the whole dataset of each region and parameter are shown in **Error! Reference source not found.**. For this specific computation, the dataset has been reduced to the records up to 10 km from the coast.

Table 2: Noise improvement ratio of the SSH / SWH / Sigma0 for each of the three Areas of Interest.

	SSH	SWH	Sigma0
Greece	81.51 %	36.5 %	25.97 %
Baltic	76.51 %	12.76 %	2.6 %
California	59.34 %	-21.18 %	-148.75 %

The highest level of noise improvement is obtained for the Greece Area of Interest, for the three geophysical estimations.

Also, we observe the SSH as the best improved parameter of the three estimations, for the three Areas of Interest.

Generally, we see a lack of Sigma0 valid retrievals for the EUMETSAT series, impacting the continuity of its representation versus distance to the coast.

Particularly in California we observe in the table a worsening of the CORS SWH and Sigma0 estimations stability with respect to EUMETSAT. If we check Figure 5 (California AoI) we can extract a different information: the SWH CORS series is stable approaching the coast up to around 4 km off-shore, when the EUMETSAT series clearly starts to increase the noise from around 7 to 8 km off-shore. The higher CORS SWH noise compared to the EUMETSAT one is concentrated in the last km. For the Sigma0, it is hard to get valid information due to the level of EUMETSAT data not represented.

The SSH noise improvement ratio is over 50% for the 3 areas, and close to 80% for Baltic and Greece, which is even better than previous validation exercises in other areas and missions. In the 3 SSH figures it is evident the wide margin of SSH noise improvement up to distances much closer to the coast: generally, we achieve at hundreds of meters from the coast the level of EUMETSAT SSH noise from around 7 km up to the coast. This is cleaning the pave of sea level Sentinel-6 science measurements reliability over several kilometres.

Area of interest: Greece

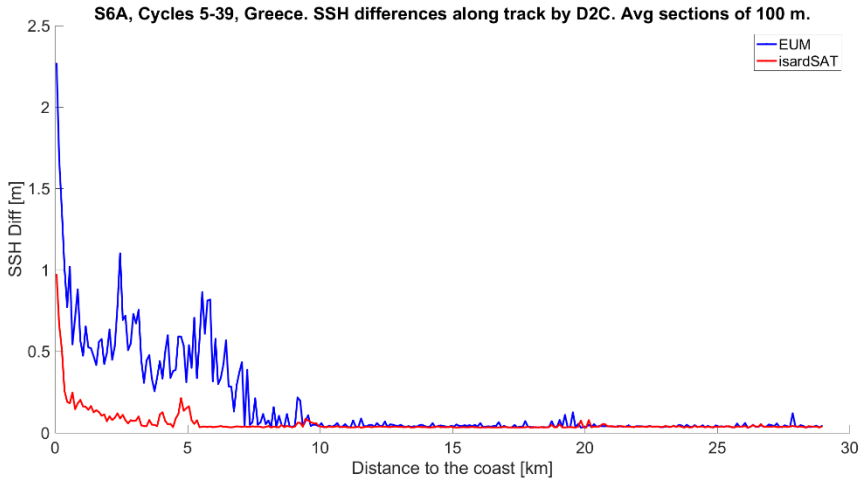

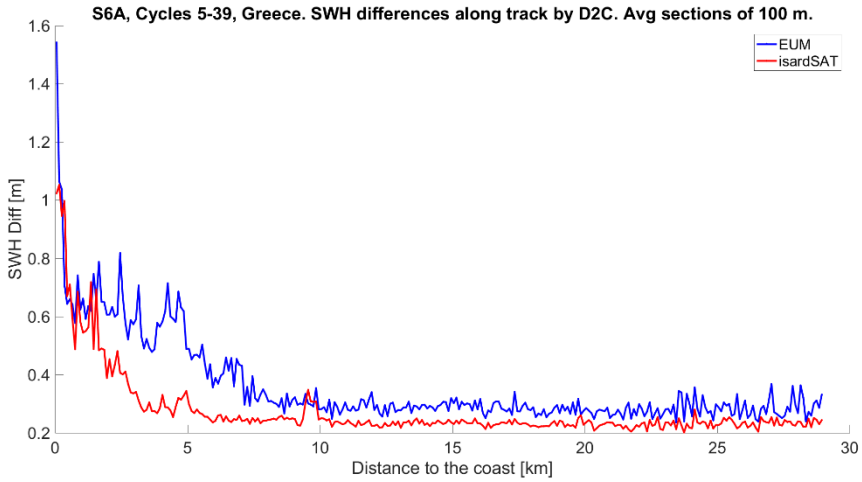

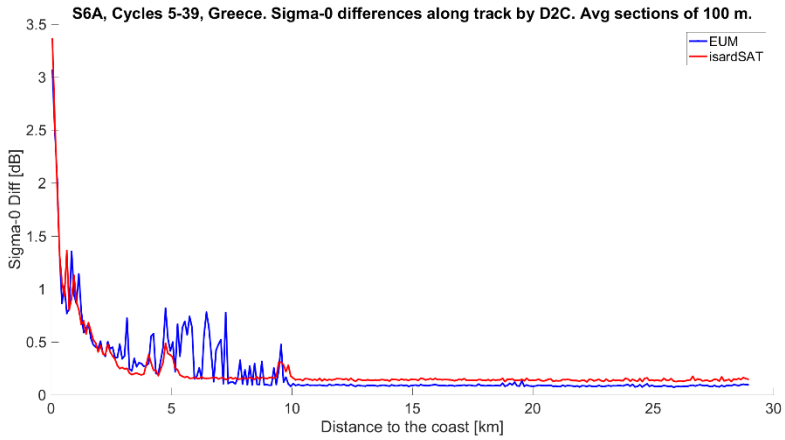

Figure 3: SSH / SWH / Sigma0 noise along track versus distance to the coast. Greece area of interest.

Area of interest: Baltic

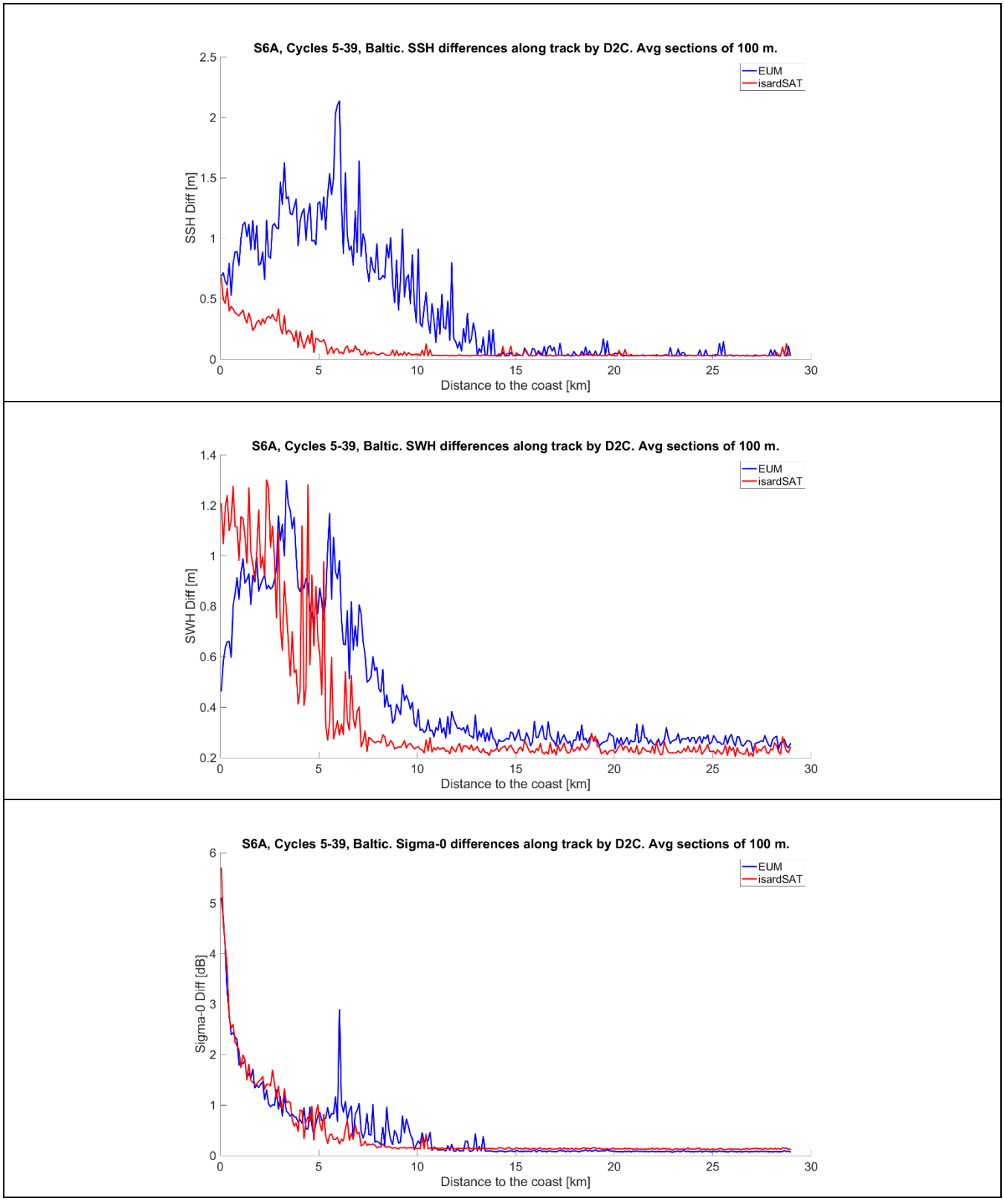

Figure 4: SSH / SWH / Sigma0 noise along track versus distance to the coast. Baltic area of interest.

Area of interest: California

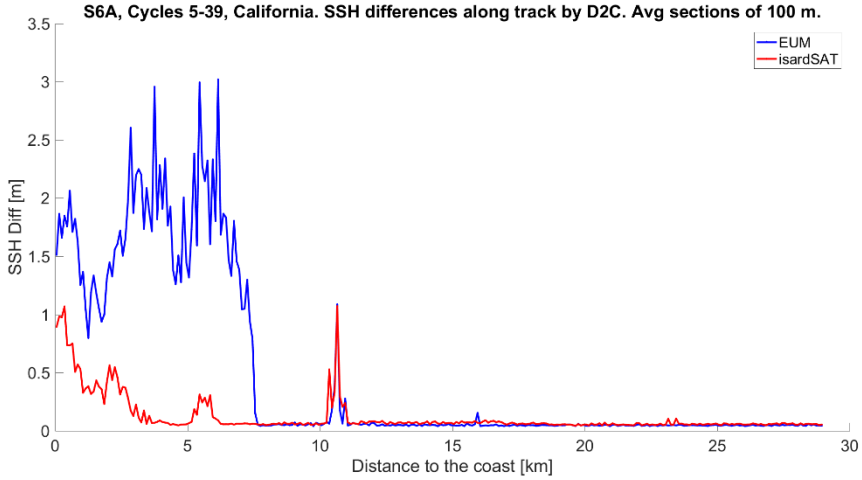

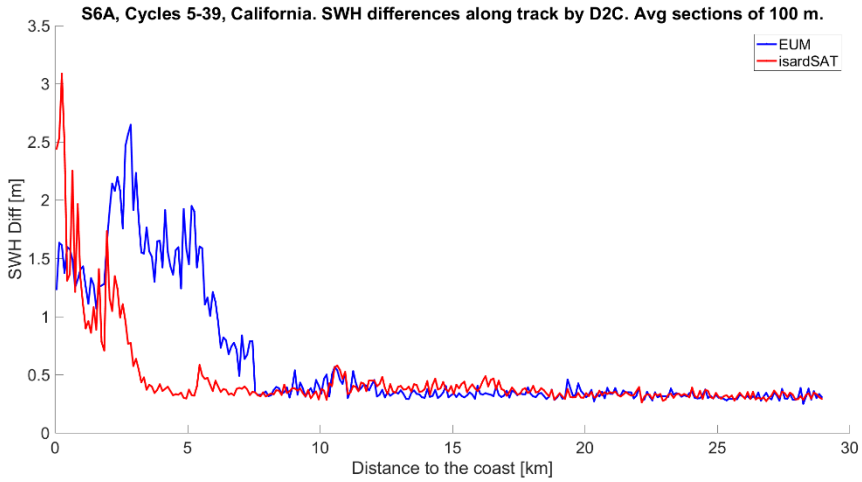

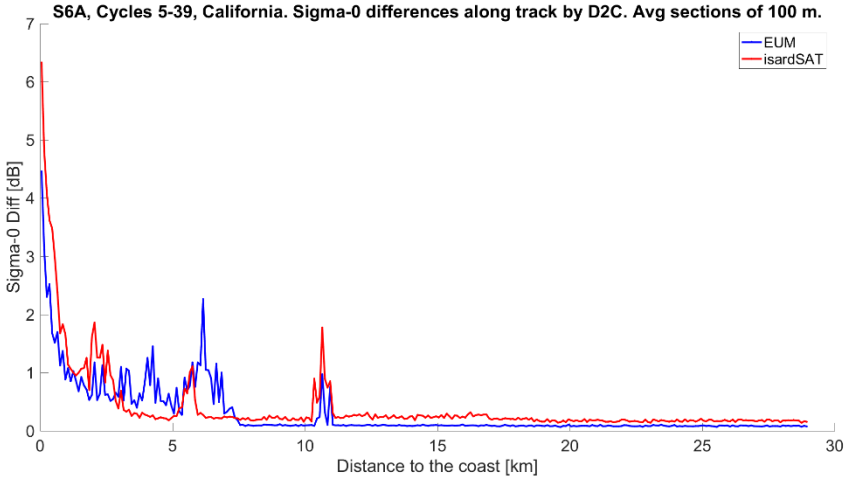

Figure 5: SSH / SWH / Sigma0 noise along track versus distance to the coast. California area of interest.

The second representation is the histogram of the three parameters (i.e., SSH, SWH & Sigma0) for a specific area of interest: Greece (Figure 6), Baltic (Figure 7) and California (

Figure 8). Each of the 3 geophysical variables have the same variable scaling in the X axis in meters or dBs, for a better intercomparison.

Again, we observe here that Greece gives the highest level of improvement, not only of CORS with respect to EUMETSAT, but also of the two products with respect of the other two AoI's: Baltic and California.

From the histograms we read the same conclusion: the SSH retrieval have better noise improvement than SWH and Sigma0. The blue (EUMETSAT) SSH along-track differences occurrences are clearly more spread than the red (CORS) ones, evidencing the high level of performance improvement. This is much more difficult (if we do) to observe in the SWH and Sigma0 histograms.

In the three SSH histograms, the CORS differences along-track are concentrated in the plus minus 5 meters region, while the EUMETSAT results are spread up to plus minus 25 to 30 meters.

The SWH histograms for Baltic and California show a more similar behaviour of the two solutions, although we can observe a persistent EUMETSAT number of occurrences for high or very high differences along-track. In the case of Greece, between 2 and 7 meters of SWH differences we see higher EUMETSAT values, with a CORS solution more concentrated in lower values (clear better CORS SWH stability).

The California Sigma0 histogram is showing higher number of occurrences of the CORS solution than the EUMETSAT one for all values of Sigma0 differences along-track. This could be related to a lack of valid measurements of the EUMETSAT dataset.

Area of interest: Greece

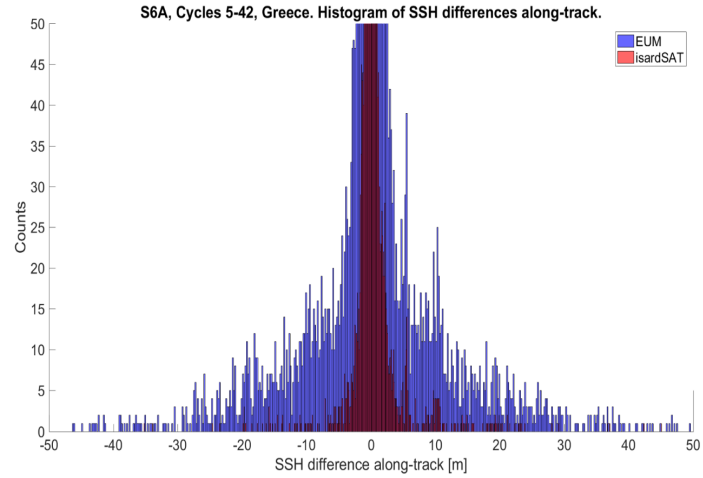

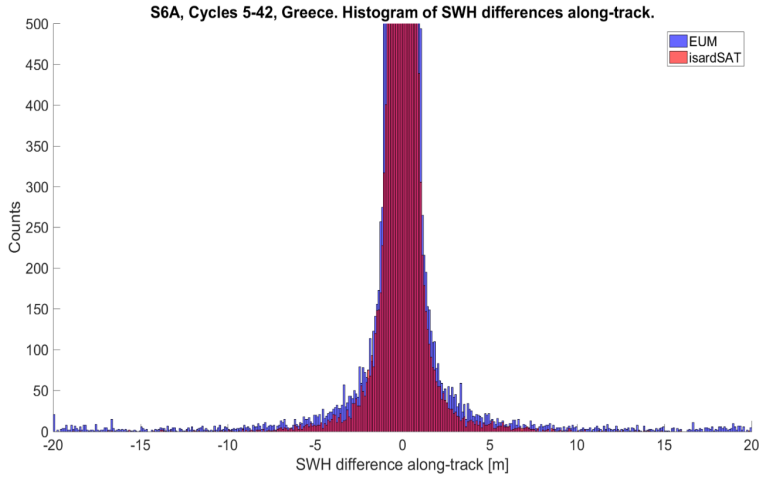

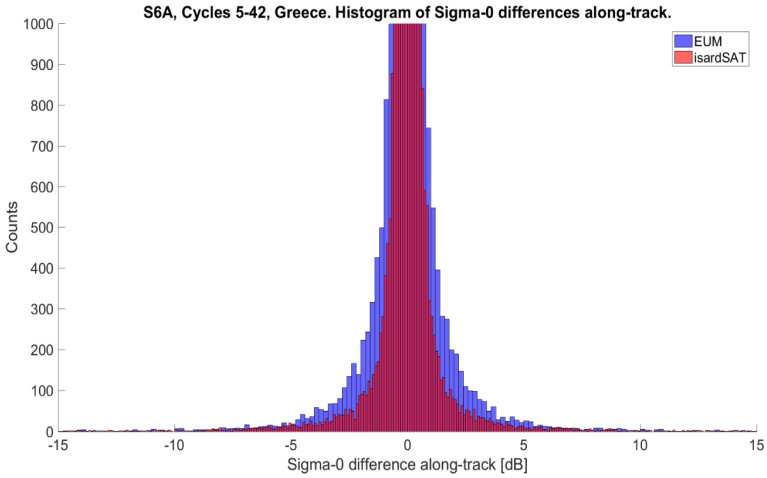

Figure 6: SSH / SWH / Sigma0 differences along-track histogram. Greece area of interest.

Area of interest: Baltic

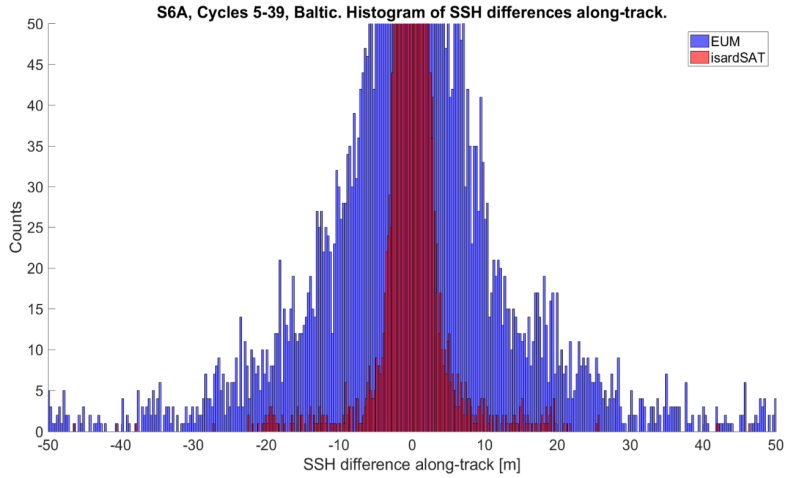

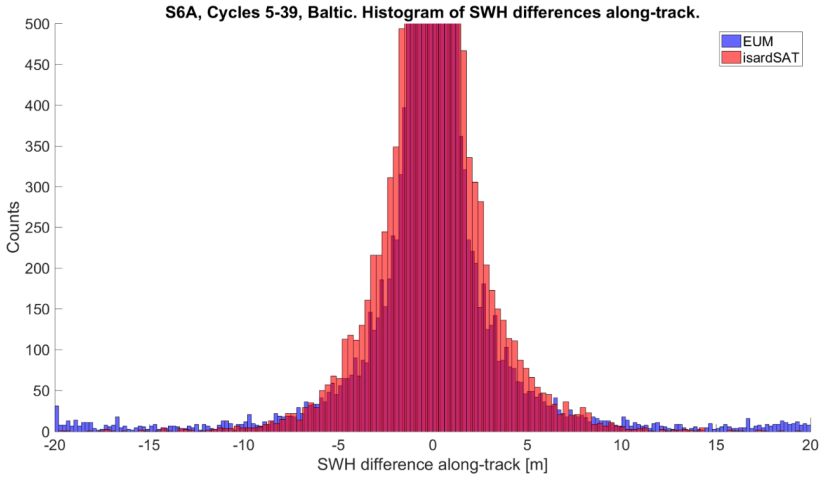

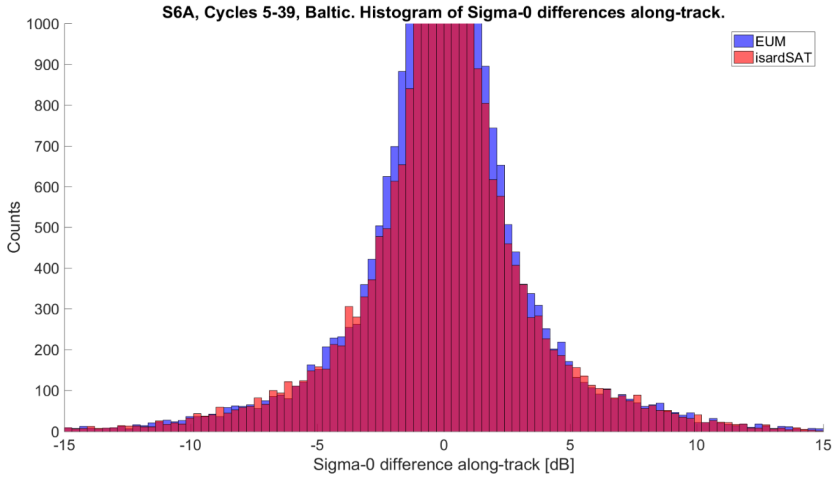

Figure 7: SSH / SWH / Sigma0 differences along-track histogram. Baltic area of interest.

Area of interest: California

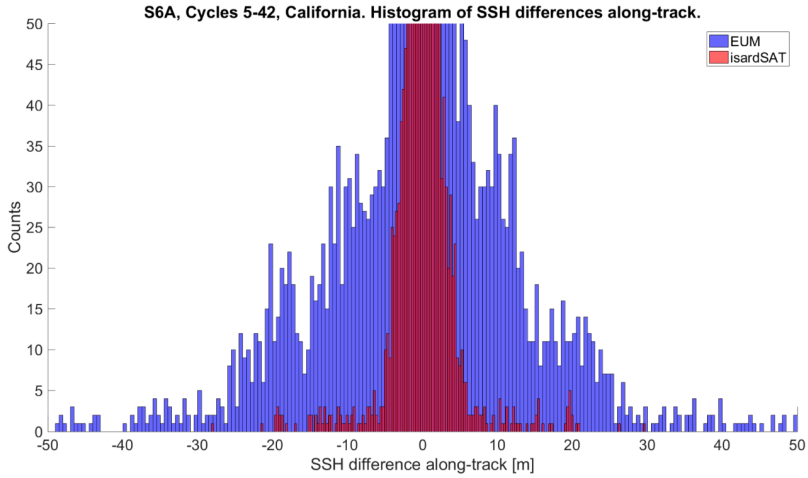

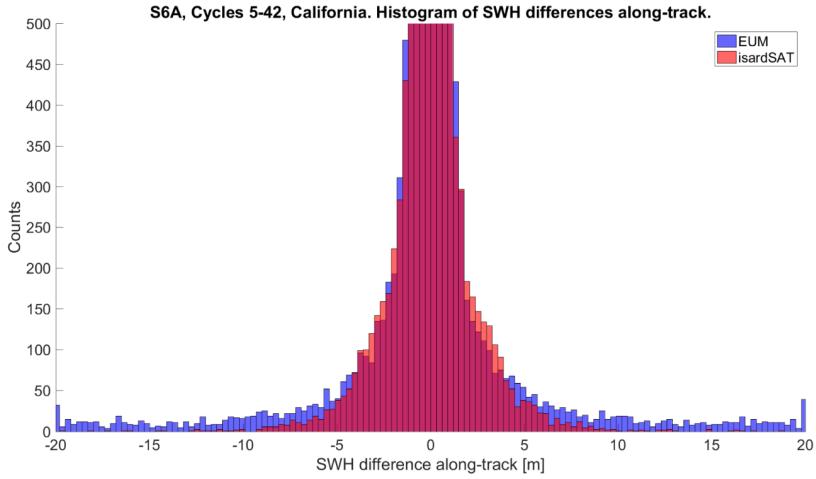

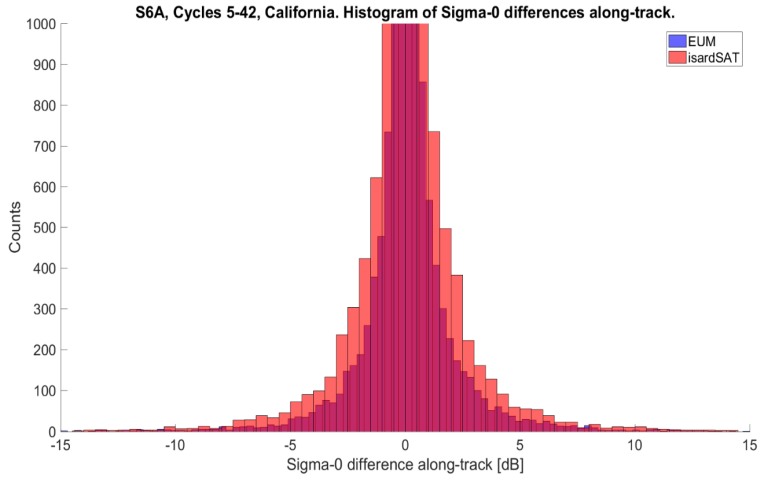

Figure 8: SSH / SWH / Sigma0 differences along-track histogram. California area of interest.

2.2.3. Power Spectral analysis.

The Power Spectral Density (PSD) plots permits to understand the amount of energy of the measured science altimeter signal, represented along the different ocean spatial scales. The wavelengths represented in the SSH and SWH PSD plots are ranging from few kilometers to some hundreds of kilometers. The approach followed for producing the plots is the same explained at (Granados, 2022), considered in the SS-CCI project.

The SSH PSD plots of the three AoI's are shown in Figure 9. The ones of the SWH parameter are shown in
Figure 10.

The plots are produced after a data filtering for avoiding anomalous Sea State conditions, which adds a considerable amount of noise to the PSD figure in form of oscillations or inconsistencies. An analysis of the dataset SWH histograms gives us the information of a very high concentration of records in the SWH filtering limits defined for each AoI plot. The California maximum SWH (5 meters) considered is higher than the Baltic and Greece ones (2.5 meters), and the lower limit is 0.5 meters for all AoI's.

The most important information we can extract from these plots is the reduction of noise along all the wavelengths of the CORS processor with respect to the EUMETSAT solution.

Usually, when analysing PSD plots, we can observe the following:

- In the longest wavelengths the different solutions lines tend to similar values, representing the real large scale ocean dynamics signal.
- In very small scales the figures also converge, as the noise represented is related to the intrinsic instrument speckle noise.
- The larger differences are usually located in the mesoscale area of the plot (5 km to tenths of kms).

The results we observe from the CORS and EUMETSAT plots are generally in agreement with the above three points. But there is a fundamental difference in the current analysis: we are observing Coastal Ocean signals, and the level of reduction of noise, especially in the SSH series, is also represented in the figures. This is why we see in the Baltic and Greece zones at almost all wavelengths a very high amount of SSH improvement in the spectra behaviour of the CORS with respect to the EUMETSAT one, a kind of result that is difficult to observe in Open Ocean analysis.

Another conclusion we can extract is that the level of improvement of the SSH noise is not that high when the SWH retrievals are higher (California). This coincides with observations in other coastal processor studies. The CORS performance over Sea Ice surfaces (Baltic in winter) is not degraded.

Also, and in agreement with the results shown in **Error! Reference source not found.**, the PSD observations of noise improvement are much better for the SSH series than for the SWH series. In the SWH case, the higher improvement is observed specifically at mesoscale regions, and proportional to the SWH: better results in higher spatial scales for higher SWH (California), and better results in lower spatial scales for lower SWH (Greece).

Power Spectral Density plot for the SSH parameter
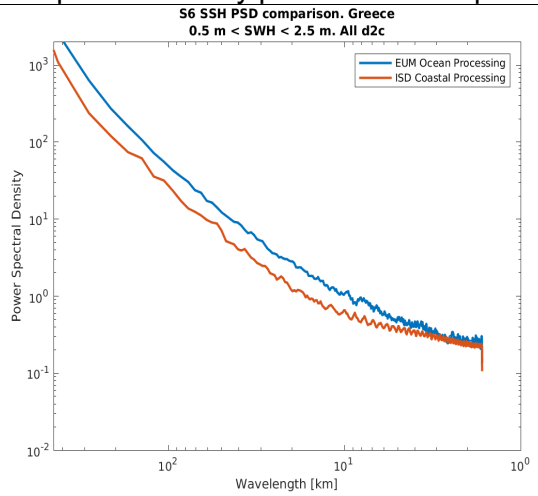
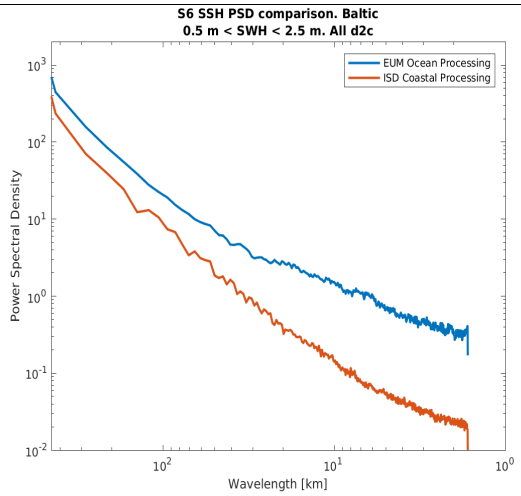
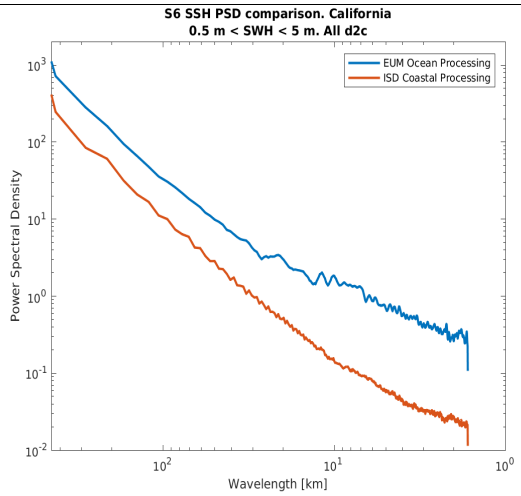

Figure 9: SSH Power Spectral Density plots for Greece, Baltic, and California areas of interest.

Power Spectral Density plot for the SWH parameter

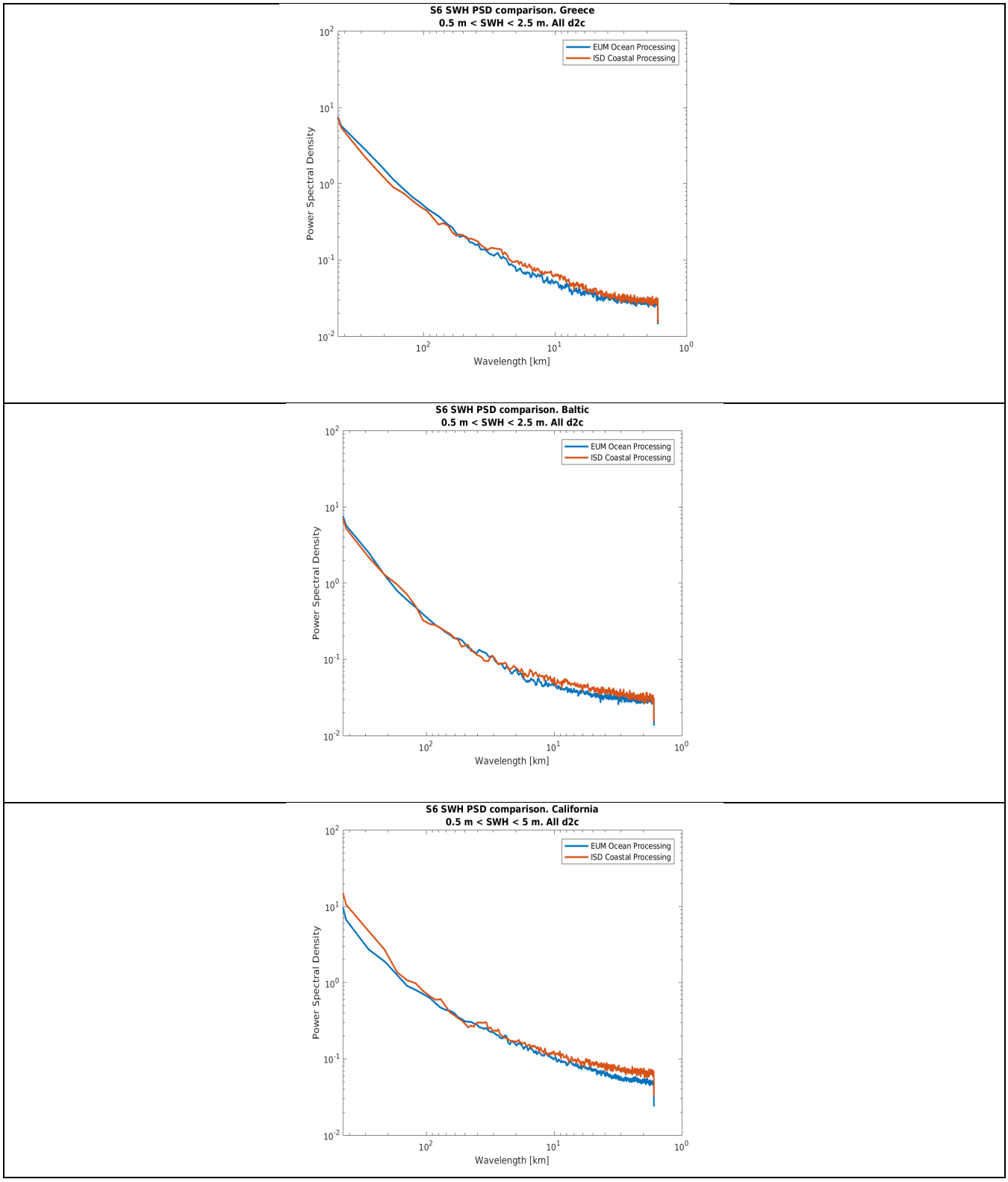

Figure 10: SWH Power Spectral Density plots for Greece, Baltic, and California areas of interest.

2.3. Conclusions

In this Coastal Ocean study, we have run the isardSAT CORS coastal processor to analyse the same coastal areas identified in the Hydrocoastal project. These are Baltic, Greece, and California. The SSH, SWH and Sigma0 CORS outputs have been compared to the L1B NTC and L2 NTC data downloaded from the EUMETSAT EO Portal.

An in-house enhanced solution for the Distance to the Coast (d2c) parameter has been designed and applied in the different validation diagnosis. It has been developed from the Open Street Map database.

From the analysis of the estimated geophysical parameters noise, we have the following outcomes:

- SSH: The best ratio of noise reduction is achieved on this parameter, from ~60 % up to more than 80% of SSH stability improvement. In general, CORS is getting at a d2c of few hundreds of meters the level of EUMETSAT SSH noise at a d2c of ~ 7 km.
- SWH: In the figures of SWH noise vs d2c, we observe a CORS improvement up to 2-3 km offshore, while from that point to the coast, it starts showing a worse behaviour.
- Sigma0: For this parameter it is hard to extract valid conclusions, due to the high amount of invalid data in the EUMETSAT products. From the figures we can see a similar behaviour.

The histograms plots are giving us a similar interpretation as the above observations.

From the Power Spectral Density (PSD) plots, the SSH is showing an outstanding improvement of the noise level at all scales and all three areas. It is worth to mention that these figures are built with only Coastal Ocean data. The SWH PSD plots are not showing a visible improvement, having CORS better results for high scales at higher SWH values and for low scales at lower SWH.

Overall, we can state that the CORS processor improves notably the S6 SSH noise up to very close to the coast, consistently in different coastal scenarios and over 1 year of data. The SWH noise show an improvement up to 2-3 km offshore. For the Sigma0, EUMETSAT products lack of valid data makes it difficult to set a conclusion.

Several evolutions of the CORS processor are envisaged, and are in implementation stage currently. They are designed to enhance the reduction of SSH noise and to bring that improvement closer to the SWH and Sigma0 parameters.

3. Sentinel-6 Fully-Focused SAR processor study on a Coastal Ocean Scenario.

This section explains the study made from the processing of 5 products of pass 94 from Sentinel-6 L1A NTC data using a Fully-Focused SAR processor. The results of such processing are analysed using different types of metrics and representations.

3.1. Overview of expected along-track resolution improvement.

In the following Figure 11, the along-track resolution improvement provided by a FF-SAR processor compared to one from a Delay-Doppler can be appreciated. Such an improvement is caused essentially by the coherent processing applied to all the pulses within the integration time in the FF-SAR processor, which is a different approach with respect to the Delay-Doppler one, where only the pulses within a burst are processed coherently, followed by an uncoherent combination of all the bursts within a similar integration time.

The scenario corresponds to an off-nadir island in the Aegean Sea on 20211222. A single-look spacing of 0.4m and multi-look of 10 m has been considered for FF-SAR processing, therefore final along-track resolutions are around 300 m for Delay Doppler and 10 m for FF-SAR.

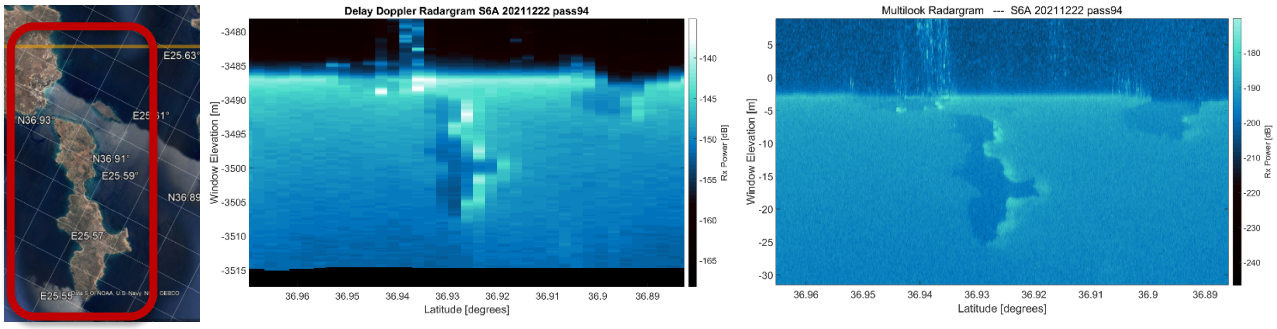

Figure 11: Area of interest with coastal scenarios (left) and examples of associated radargrams obtained with Delay Doppler (middle) and FF.SAR (right)

Just to provide a more illustrative example, Figure 12 provides an view of radargram collocated with ground track optical image showing how different features such as coast entries and nearby islands appear in the radargram.

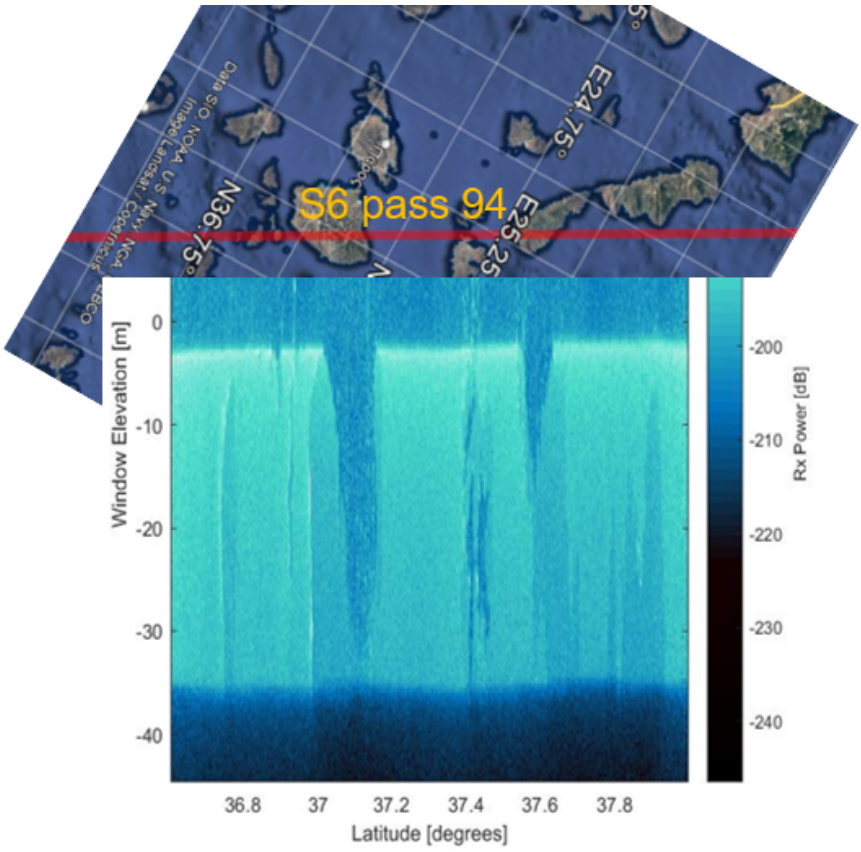

Figure 12: Example of radargram associated to the Sentinel-6 pass 94 on an area with high density of coastal areas and islands.

3.2. Input Data and Area of Interest

For the Fully-Focused study, we use the Sentinel-6 pass relative number 94 around the end of year 2021, from cycle 37 to cycle 41. The pass 94 was selected from all the passes over the Aegean Sea, due to its interest in terms of number of coastal fronts and scenarios. It covers different cases of coastal angles of attack, crossing the coast or passing close to it, lower or higher elevations of land topography close to the coast, etc. Also, this same pass presents an interesting section over Open Ocean while approaching Egypt.

The official ground track of the pass 94 is shown in the following Figure 13. The coastal section under study is between latitudes 36.6 and 38 North, as indicated in the figure.

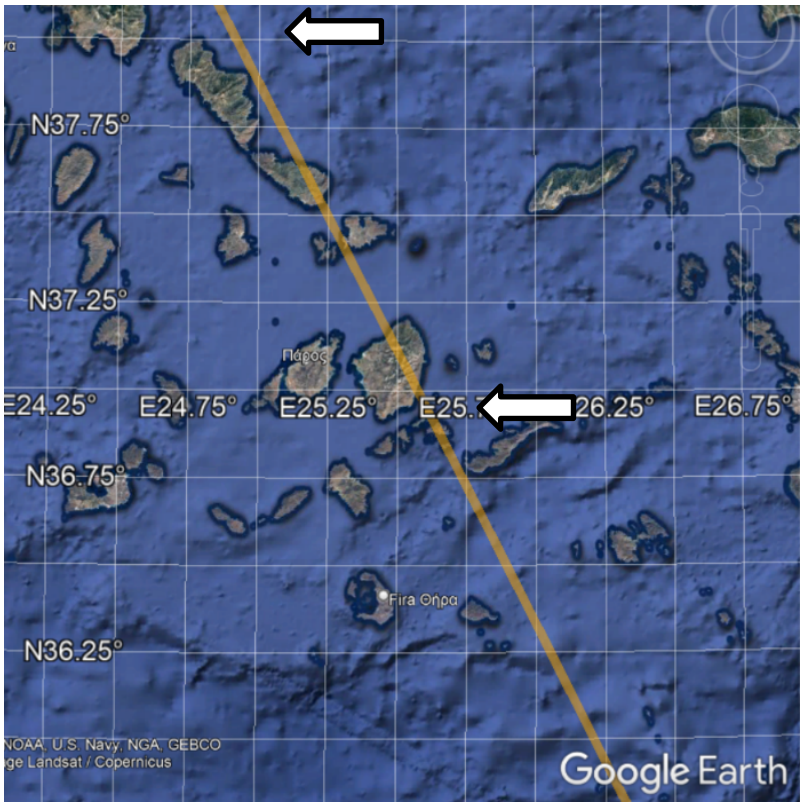

Figure 13: Sentinel-6 pass94 across the Aegean Sea, where multiple islands are crossed.

The original data for the study was downloaded from the EUMETSAT EO Portal, and consist in L1A, L1B and L2 NTC products. From it we have performed the Fully-Focused SAR processing as explained in the next section.

3.3. Methodology

The methodology is split into three steps:

1. FF-SAR processing from L1A to L1B-FF.
2. Adaptation of the retracker to operate with FF-SAR waveforms.
3. Description of the different analysis carried out and the external products used for validation and comparison.

3.3.1. From L1A to L1B: FF-SAR processor

The FF-SAR processor is part of the S6-GPP processor developed by isardSAT and based on the backprojection method [Egido, 2016]. To cope with the specific needs of the Hydrocoastal project investigation, a number of configuration parameters has been modified. The flexibility of the isardSAT processor in that regard makes it possible to use it without changing the algorithms approach.

The main configuration options considered are defined in Table 3.

Table 3: FF-SAR processing baseline configuration considered.

Parameter	Description	Value
Integration time	Time length considered for selecting the number of pulses processed for each Single-Look waveform	4.75 s
Range zero-padding	Zero-padding in range dimension	2
Single-Look Spacing	Along-track distance between focussed surfaces	0.4 m
Multi-look spacing	Multi-look in power in the along-track direction	10 m / 300 m

3.3.2. From L1B to L2: Analytical Coastal retrackers

The adaptation in terms of post-L1B processing is simple, as it does not present main differences with respect to the Delay Doppler CORS processing. Minor format adaptations have been taken into account, but the core idea is the same: retrieve a section of the waveform to be retracked, based on computing the expected coastal ocean surface elevation from the unbiased MSS over Open Ocean, projected towards the coastline.

The parameters were retracked from FFSAR waveforms by fitting the DD multilook model waveform in (Ray et al., 2015; Makhoul et al., 2018). The multilook model waveforms resulted from the incoherent averaging of a full-stack model with a fixed number of contributing beams per surface location. The look angles corresponding to the contributing beams were estimated from the coherent integration time of the FFSAR processing, the altitude, the satellite velocity at the surface location and the angular beam azimuth resolution. Because FFSAR waveforms resemble a nadir-looking beam, prior to model stack multilooking, the contribution of outer beams is mitigated by the application of a Doppler mask based on the slant range correction.

3.3.3. Data analysis scheme

In order to validate FF-SAR products in coastal areas we have taken into account different products

1. L2 Delay Doppler from EUMETSAT
2. L2 Delay Doppler from isardSAT
    - Based on L1B NTC from EUMETSAT
3. L2 Delay Doppler coastal from isardSAT
    - Based onL1B NTC from EUMETSAT, adding CORS processing.
4. L2 FF-SAR from isardSAT
    - Based on L1A NTC from EUMETSAT
    - Processed to L1B FF-SAR with the S6 GPP FF-SAR processor (developed by isardSAT).
5. L2 FF-SAR coastal from isardSAT
    - Based on L1A NTC from EUMETSAT
    - Processed to L1B FF-SAR with the S6 GPP FF-SAR processor (developed by isardSAT), adding CORS processing.

- Finally, three analyses have been conducted within this study:
    1. An overall along track noise analysis
    2. A noise vs. distance to coast analysis
    3. An open ocean vs. coastal area retracker performance area.

3.4. Along track noise analysis

The along track noise analysis evaluates the absolute performance of each L2 products corresponding to the date 22/12/2021 for each geophysical retrieval: SSH, SWH and Sigma0. Three cases have been considered:
(a) FF-SAR averages every 300 m, to approximately match the same sampling as DD,
(b) FF-SAR averages every 100 m and, finally,
(c) FF-SAR averages every 50 m, to assess the performance of the same parameters but at higher along-track sampling.

The figures of merit are the standard deviation of each parameter in the series considered, and the mean of the diff() of each parameter as well.

A final summary of this analysis is presented at the end of the section.

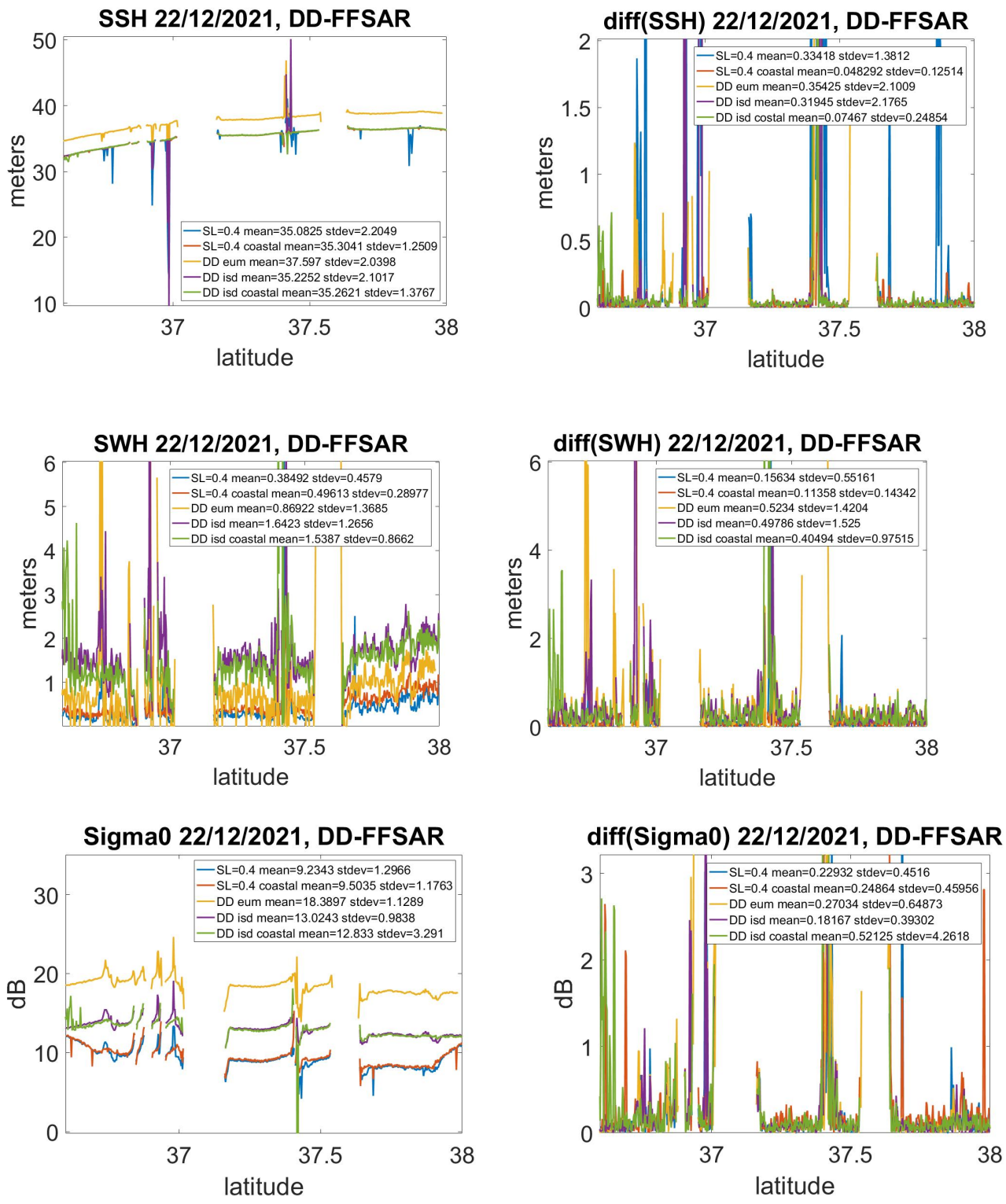

Figure 14:: Case (a) SSH, SWH and Sigma0 with FF-SAR averaged every 300 m

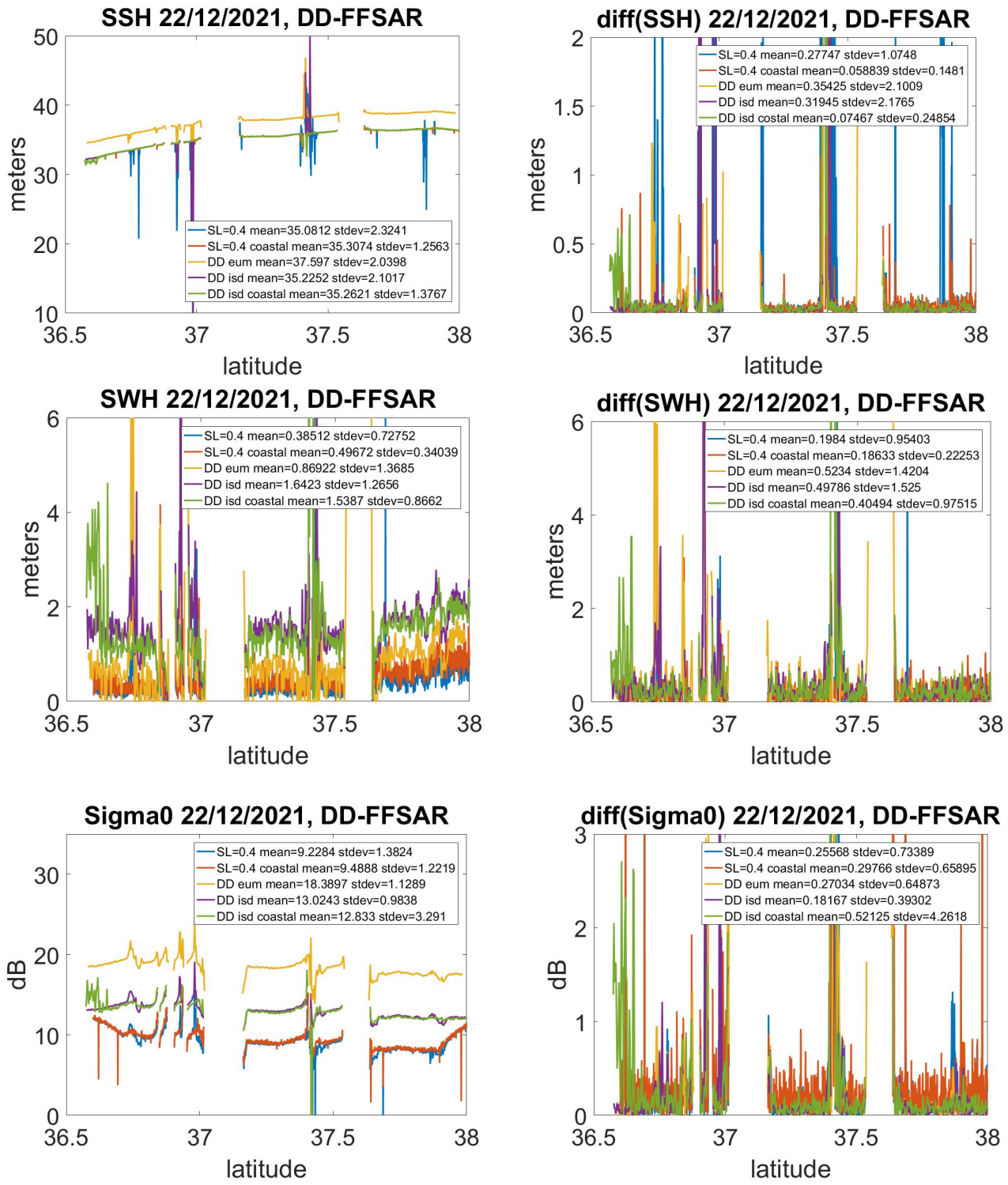

Figure 15: Case (b) SSH, SWH and Sigma0 with FF-SAR averaged every 100 m

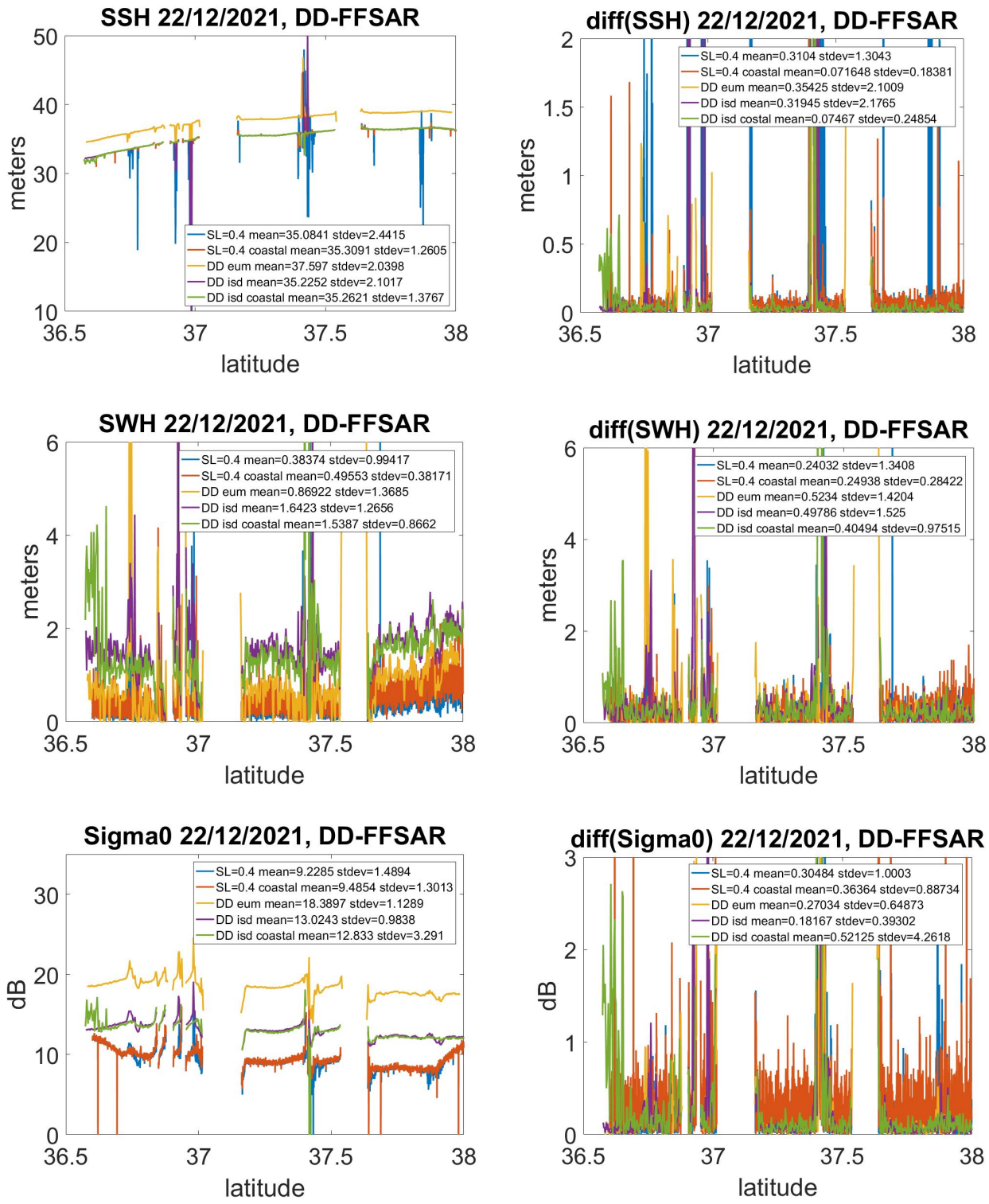

Figure 16: Case (c) SSH, SWH and Sigma0 with FF-SAR averaged every 50 m

The following tables provide a summary of results of the along track noise analysis.

First, the benefit of using the coastal retracker on DD data compared to a generic ocean one is demonstrated in the first three raws in Table 4, specifically on SSH and SWH, where the isardSAT (ISD) coastal retracker shows a better performance compared to EUM and isardSAT's analytical ocean retrackers. Secondly, in Table 4 it is shown as well that FF-SAR data with coastal retracker is able to notably improve the DD performance on SSH and SWH at an along-track spacing of 300 m, equivalent to the one from DD.

Finally, Table 5 shows that the previous FF-SAR improvement with respect to Delay-Doppler data is not achieved only at an equivalent spacing of 300 m, but also at the smaller spaces of 100 m and 50 m. Small degradation is observed at the smaller spaces, but still above DD performances.

Table 4: Summary of DD/FF-SAR performances on the along track noise analysis for comparison.

Products	SSH [m] (std)	diff(SSH) [m] (mean)	Sigma0 [dB] (std)	diff(Sigma0) [dB] (mean)	SWH [m] (std)	diff(SWH) [m] (mean)
DD EUM	2.0398	0.3543	1.1289	0.2703	1.3685	0.5234
DD ISD Ocean	2.1017	0.3195	0.9838	0.1817	1.2656	0.4979
DD ISD Coastal	1.3767	0.0747	3.2910	0.5213	0.8662	0.4049
FF ISD Ocean SL=0.4 ML=10 (Average every 300 m)	2.2049	0.3342	1.2966	0.2293	0.4579	0.1563
FF ISD Coastal SL=0.4 ML=10 (Average every 300 m)	1.2509	0.0483	1.1763	0.2486	0.2898	0.1136

Table 5: FF-SAR processed data results with the Coastal retracker on the along track noise analysis

Products	Average every	SSH (mean, std)	diff(SSH) (mean)	Sig0 (mean, std)	diff(Sig0) (mean)	SWH (mean, std)	diff(SWH) (mean)
FF ISD Coastal SL=0.4 ML=10	300 m	35.3041, **1.2509**	0.0483	9.5035, **1.1763**	0.2486	0.4961, **0.2898**	0.1136
	100 m	35.3074, 1.2563	0.0588	9.4888, 1.2219	0.2977	0.4967, 0.3404	0.1863
	50 m	35.3091, 1.2605	0.0717	9.4854, 1.3013	0.3636	0.4955, 0.3817	0.2494

3.5. Noise vs distance to coast

In this section we evaluate the noise at different distances to the coast considering 5 tracks. The different passes analysed are the ones from cycles 37 to 41.

The noise improvement ratio is defined here as the relation between any DDP-isardSAT or FF-SAR solution with respect to DDP-EUMETSAT. The ratio is obtained by dividing the difference between the two datasets by the DDP-EUMETSAT value.

The FF-SAR options with single-look spacing of 0.4 m and two different multi-looking lengths of 10 m and 300 m have been considered for this analysis. For each case, both the ocean and coastal retrackers have been applied.

With a distance section length of 100 m, the noise improvement ratios obtained are shown in Figure 17.

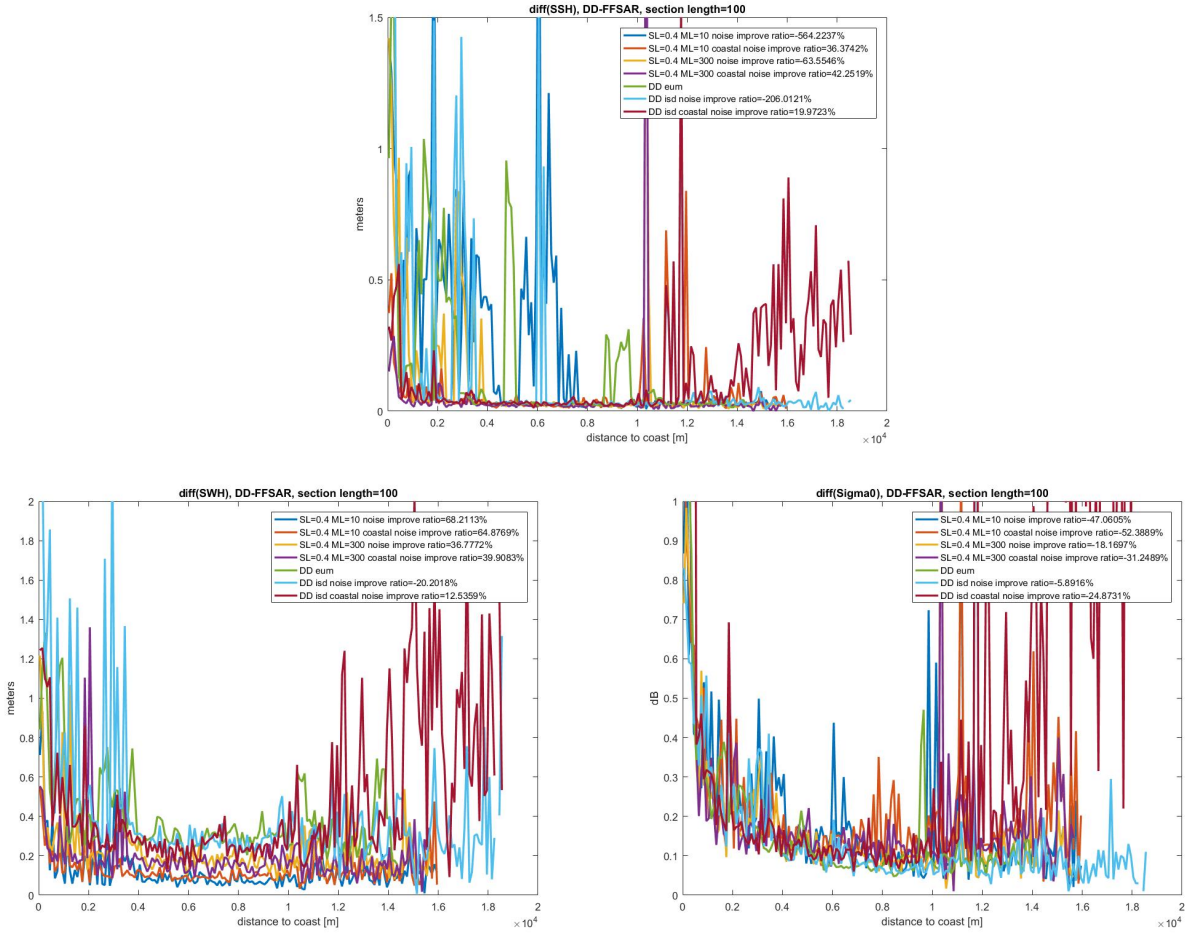

Figure 17: Improvement rations for SSH, SWH and Sigma0 without removing outliers.

Note that noise at high distances to coast are noisy basically due to the low number of passes included in the analysis (low population of those 100 m bins). Such analysis would benefit from including a much larger number of passes or longer periods of time, for instance considering the whole Mediterranean Sea for one month, much clearer figures would be obtained.

Results here show a better improvement ratio of all SSH computations when using the coastal processor with respect to the case using the open ocean retracker. FF-SAR and DD coastal improves current L2-EUM results by roughly 40% and 20% respectively. No improvement is achieved for the ocean analytical retracker.

Regarding SWH, the improvement is more significant: from 37% to 65% in FF-SAR, and around 13% in DDP, all of them using the coastal retracker. Still, for this parameter the ocean analytical retracker yields strong improvements, from 40% to 68% in FF-SAR, although worsening in the case of DD.

Finally, no sigma0 improvement is achieved for any of the retrackers, confirming the fact that the current version of the retracker needs still some work on evolutions in terms of amplitude retrievals.

3.5.1. Summary

A summary of results on the along-track noise analysis is presented in Table 6. It must be remarked that the FF-SAR processor provides strong improvement with the coastal retracker for both SSH and SWH, at a strongly improved along-track resolution of 10 m. Notable improvements are obtained when using the ocean retracker but only in terms of SWH.

Table 6: Summary of DD / FF-SAR performances on the distance to coast analysis. Only positive improvement ratios with respect to L2-EUM results are included.

Along track noise	Processor	Multi-looked	Retracker	Improvement ratio wrt L2-EUM	
				SSH	SWH
	FF-SAR	10 m	Coastal	36.4	64.9
			Ocean	--	68.2
		300 m	Coastal	42.3	36.8
			Ocean	--	39.9
	DDP		Coastal	20.0	12.5
			Ocean	--	--

3.6. Open Ocean performance vs. Coastal area

The performance of the FF-SAR processed data is here evaluated in open ocean to compare its performance against coastal areas, and also with different Delay-Doppler solutions:

- Delay-Doppler from EUMETSAT
- Delay-Doppler from isardSAT, with the ocean retracker
- Delay-Doppler from isardSAT, with the coastal retracker

Regarding the FF-SAR product, in this case, no averages are applied, and results are provided directly with final multi-looked spacings of either 10 m or 300 m.

A 200 km segment of data close to Egypt as part of the Sentinel-6 pass 94, with latitudes up to 32.5N, has been used as an open ocean scenario.

The following figures provide the results of the three cases considered:

- Figure 18: SSH, SWH and Sigma0 on an open ocean segment retracked with the ocean retracker.
- Figure 19: SSH, SWH and Sigma0 on a coastal segment retracked with the ocean retracker.
- Figure 20: SSH, SWH and Sigma0 on a coastal segment retracked with the coastal retracker.

Finally, Table 7 provides a summary of performances for the different cases considered. In first place, it can be observed that FF-SAR over ocean and averaged every 300 m slightly improves current DD-based performances for SSH and SWH. Instead, the improvement over a coastal segment retracked with the same ocean retracker is much higher. However, when applying the coastal retracker on the coastal segment, the best SSH performance is achieved by the DD L2 isardSAT product, while the best SWH is achieved by the FF-SAR dataset. In terms of along-track resolution, the 10-m case does not provide any additional improvement with respect to the 300 m case for this dataset.

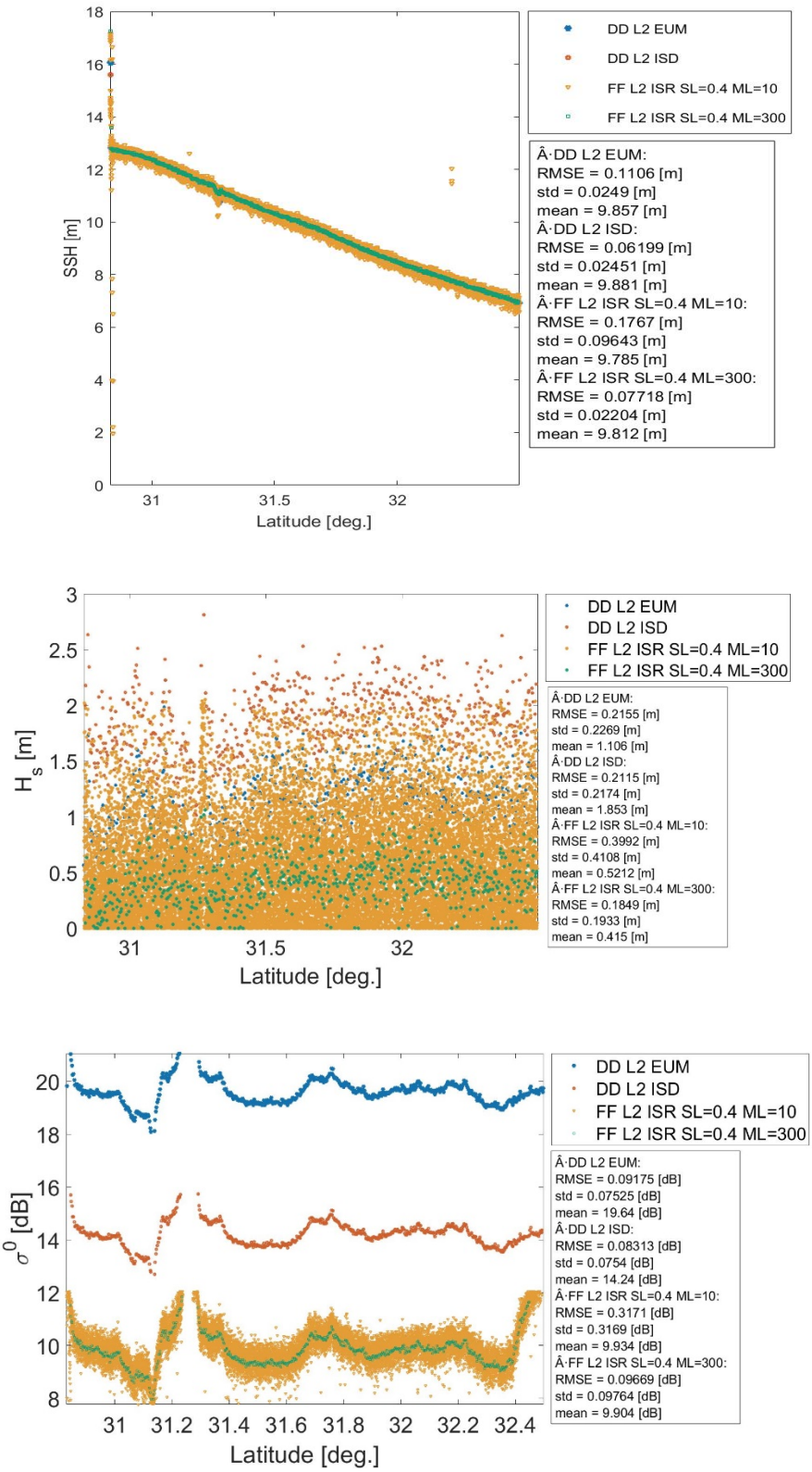

Figure 18: SSH (with zoom), SWH and Sigma0 on an open ocean segment retracked with the ocean retracker.

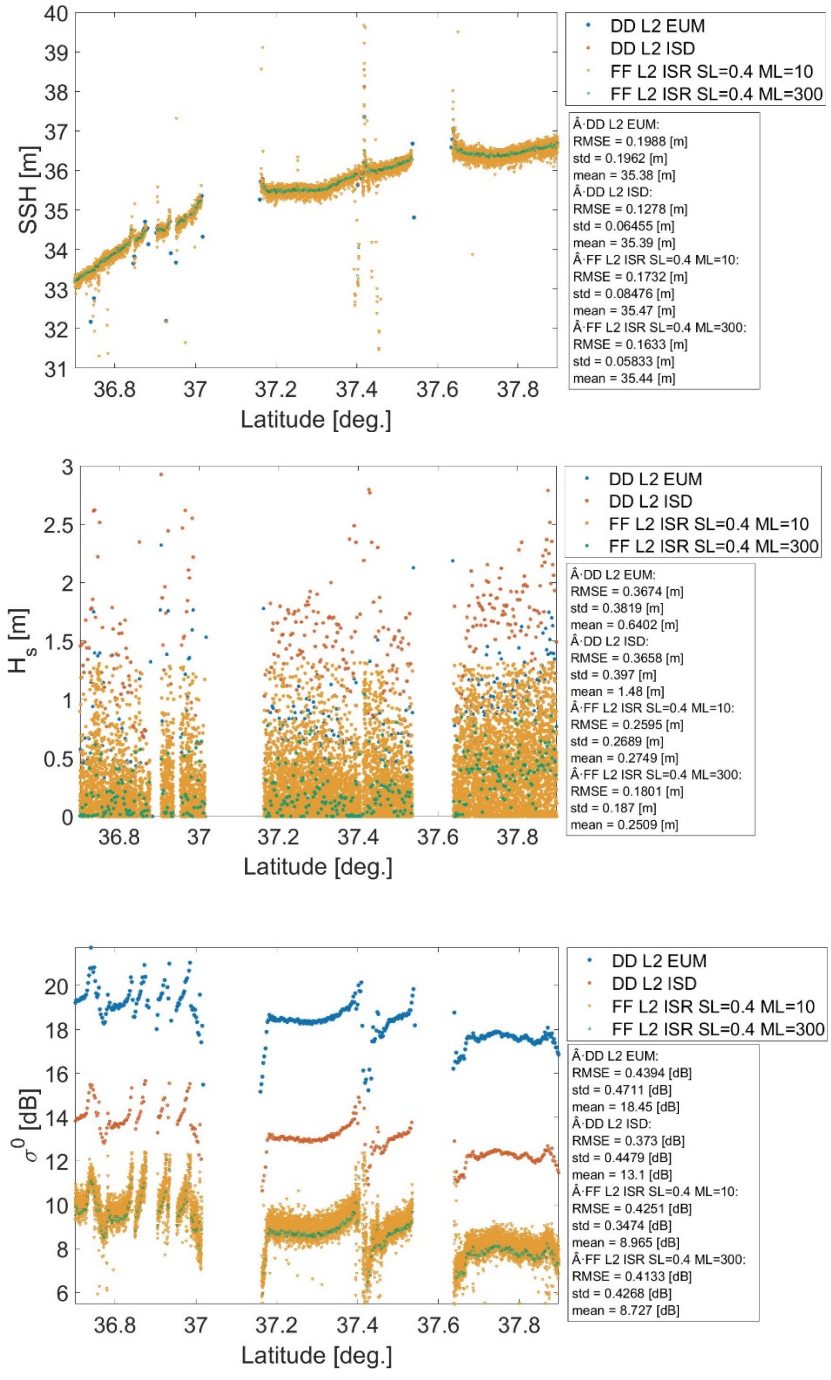

Figure 19: SSH, SWH and Sigma0 on a coastal segment retracked with the ocean retracker.

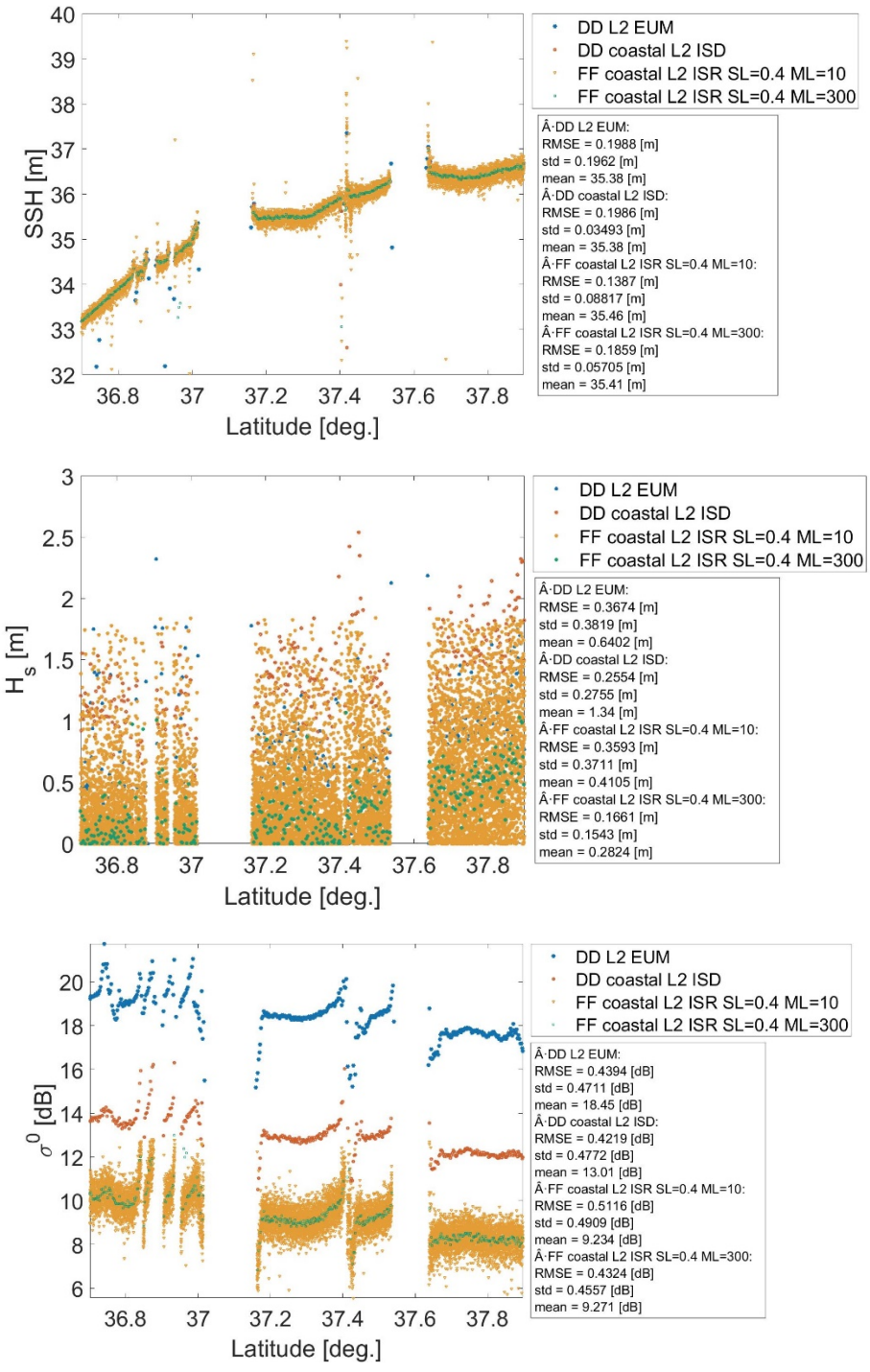

Figure 20: SSH, SWH and Sigma0 on a coastal segment retracked with the coastal retracker.

Table 7: Summary of performances over open ocean with the analytical ocean retracker and over a coastal area retracked with either the same analytical ocean retracker and with the coastal retracker, both for DD and FF-SAR.

	Products	Std SSH [m]	Std σ^0 [dB]	Std Hs [m]
Open Ocean with Ocean Retracker	DD L2 EUM	0.0249	0.0753	0.2269
	DD L2 ISD	0.0245	0.0754	0.2174
	FF L2 ISD SL=0.4 ML=300	0.0220	0.0976	0.1933
Coastal with Ocean Retracker / Coastal Retracker	DD L2 EUM	0.1962	0.4711	0.3819
	DD L2 ISD	0.0646 / 0.0349	0.4479 / 0.4772	0.3970 / 0.2755
	FF L2 ISD SL=0.4 ML=300	0.0583 / 0.0571	0.4268 / 0.4557	0.1870 / 0.1543

3.7. Conclusions

This study has demonstrated that FF-SAR data over coastal areas, specifically that retracked with dedicated coastal retrackers, not only exceed the current performances achieved by operational Delay-Doppler processing, but also is able to improve the along-track resolution at least to a factor 6 (to 50 m) without much degradation.

In terms of along-track noise, FF-SAR data retracked with the coastal retracker reports improved results for SSH and SWH with respect to any L2 DD-based solution.

Also in terms of distance to coast performance, the FF-SAR data retracked with the isardSAT coastal retracker is able to improve retrievals up to about 36% in SSH and 65% in SWH at an improved along-track resolution of 50 m. If data outliers are removed from the series, the SWH improvement ratio is still the same though the SSH ration decays to a 14% of improvement.

A test done over ocean shows that FF-SAR data with ocean retracker is able to improve DD-based SSH and SWH estimates only when averaged at a 300 m, and also improves performances over coastal areas when using the ocean retracker, while over coastal areas retracker with the coastal retracker the best SSH performance is achieved by the DD L2 isardSAT retracker and only the best SWH performance is achieved by the FF-SAR.

Still, such improvements have only been demonstrated so far in SSH and SWH retrievals, as the current implementation of the coastal retracker is likely to fail in the estimation of Sigma0 and should be improved. A two-step retracking strategy (Gao *et al.*, 2019) adapted to coastal waveforms is expected to improve the estimation of Sigma0. This approach enforces a secondary fitting procedure when the quality of the primary fitting of the three parameters SWH, SSH and Sigma0 is low, especially for specular reflections. This secondary fitting is performed over the parameters SSH, Sigma0 and mean squared slopes (MSS) describing the sea surface roughness, given a fixed value for SWH.

Significant performance improvements provided by FF-SAR data retracked with specific coastal retrackers, compared to current DD-based products, have been demonstrated. Still, the analysis presented has been limited to the specific scope of this HYDROCOASTAL CCN and we would thus recommend to continue this analysis in the future in order to provide a more detailed understanding of the FF-SAR benefits over coastal areas.

4. References

Buchhaupt et al. (2018): A fast convolutional based waveform model for conventional and unfocused SAR altimetry. ASR, 62(6), 1445-1463, https://doi.org/10.1016/j.asr.2017.11.039.

Egido, Alejandro & Smith, Walter. (2017). Fully Focused SAR Altimetry: Theory and Applications. IEEE Transactions on Geoscience and Remote Sensing. PP. 1-15. 10.1109/TGRS.2016.2607122.

Gao, Q., Makhoul, E., Escorihuela, M., Zribi, M., Quintana Seguí, P., García, P. & Roca, M. (2019). Analysis of Retrackers' Performances and Water Level Retrieval over the Ebro River Basin Using Sentinel-3. *Remote Sensing of Environment*, 11(6):718. https://doi.org/10.3390/rs11060718

García, Pablo; Martin-Puig, Cristina; Roca, Mònica. SARIn mode, and a window delay approach, for coastal altimetry, Advances in Space Research, Volume 62, Issue 6, 2018. https://doi.org/10.1016/j.asr.2018.03.015

Granados, A. ACDC retracking of Round Robin S3A dataset Climate Change Initiative - Sea State WP 2000, ESA SS-CCI TN, June 3, 2022.

Jiang, L., Nielsen, K., Dinardo, S., Andersen, O.B., Bauer-Gottwein, P. (2020): Evaluation of Sentinel-3 SRAL SAR altimetry over Chinese rivers, Remote Sensing of Environment, *237*, 111546, https://doi.org/10.1016/j.rse.2019.111546.

Makhoul, E., Roca, M., Ray, C., Escolà, R., & Garcia-Mondéjar, A. (2018). Evaluation of the precision of different Delay-Doppler Processor (DDP) algorithms using CryoSat-2 data over open ocean. *Advances in Space Research*, *62*(6), 1464-1478.

Ray, C., C. Martin-Puig, M. Clarizia, G. Ruffini, S. Dinardo, C. Gommenginger, and J. Benveniste (2015), "SAR Altimeter Backscattered Waveform Model," IEEE Transactions on Geoscience and Remote Sensing, vol. 53, no. 2, pp. 911–919, 2015

Roscher et al. (2017): STAR: Spatio-temporal altimeter waveform retracking using sparse representation and conditional random fields. *RSE*, 201, 148-164, https://doi.org/10.1016/j.rse.2017.07.024.

Villadsen, H., Deng, X., Andersen, O.B., Stenseng, L., Nielsen, K. & Knudsen, P. (2016): Improved inland water levels from SAR altimetry using novel empirical and physical retrackers, *Journal of Hydrology, 537*, https://doi.org/10.1016/j.jhydrol.2016.03.051

5. List of Acronyms

ACE2	Altimeter Corrected Elevations (vers. 2)
AD	Applicable Documents
AGC	Automatic Gain Control
AH	Alti-Hydro
AHP	Alti-Hydro Product(s)
AI	Action Item
AIM	Action Item Management (tool)
AltiKa	Altimeter in Ka band and bi-frequency radiometer instrument
AMSR-E	Advanced Microwave Scanning Radiometer-Earth Observing System
ANA	Agência Nacional de Águas (National Water Agency, Brazil)
AoA	Angle of arrival
API	Application Programming Interface
AR	Acceptance Review
ASAP	As Soon As Possible
ASCII	American Standard Code for Information Interchange
ATBD	Algorithm Technical Basis Document
ATK	Along-Track S.A.S.
AVISO	Archivage, Validation et Interprétation des données des Satellites Océanographiques
BIPR	Background Intellectual Property Right
CASH	Contribution de l'Altimetrie Spatiale à l'Hydrologie (Contribution of Space Altimetry to Hydrology)
CCN	Contract Change Notice
CFI	Customer Furnished Item
CLASS	NOAA/Comprehensive Large Array-Data Stewardship System
CoG	Centre of Gravity
CPP	CryoSat-2 Processing Prototype (CNES)
CryoSat-2	Altimetry satellite for the measurement of the polar ice caps and the ice thickness
CRISTAL	Copernicus polaR Ice and Snow Topography ALtimeter
CRUCIAL	CRyosat-2 sUCcess over Inland wAter and Land
CSV	Coma Separated Values
CTOH	Centre de Topographie des Océans et de l'Hydrosphère (Centre of Topography of the Oceans and the Hydrosphere)
DAO	Data Access Object
DARD	Data Access Requirement Document
DDM	Delay-Doppler Map
DDP	Delay-Doppler Processor
DEM	Digital Elevation Model
DGC	Doppler Ground Cell
DPM	Detailed Processing Model
DPP	Data Procurement Plan
DTC	Dry Tropospheric Correction
DTU	Danmarks Tekniske Universitet (Technical University of Denmark)
DVT	Data Validation Table
ECMWF	European Centre for Medium-Range Weather Forecasts
ECSS	European Cooperation for Space Standardisation
EGM	Earth Gravitational Model
ENVISAT	ENVIronment SATellite
EO	Earth Observation
EOEP	Earth Observation Enveloppe Programme
EOLi	Earth Observation Link
EOLi-SA	EOLi-Stand Alone
EPN	EUREF Permanent Network
ERA	ECMWF ReAnalysis
ESA	European Space Agency
EUREF	IAG Reference Frame Sub-Commission for Europe
FBR	Full Bit Rate
FFT	Fast Fourier Transform
FR	Final Review
FTP	File Transfer Protocol
FCUP	(from portuguese) *"Faculdade de Ciências da Universidade"*, Science faculty of the University of Porto
GDAL	Geospatial Data Abstraction Library
GDR, [I-,S-]	Geophysical Data Record, [Interim-, Scientific-]
GFZ	Deutsche GeoForschungsZentrum (German Research Centre for Geosciences)
GNSS	Global Navigation Satellite System

GOCE	Gravity field and steady-state Ocean Circulation Explorer
GPD	GNSS-derived Path Delay
G-POD	Grid Processing on Demand
GPT2	Global Pressure and Temperature model (vers. 2)
GPP	Ground Processing Processor
GPS	Global Positioning System
GRACE	Gravity Recovery And Climate Experiment
GRDC	Global Runoff Data Centre
GRGS	Groupe de Recherche de Géodésie Spatiale (Space Geodesy Research Group)
GRLM	Global Reservoir and Lake Monitor
GTN-L	Global Terrestrial Network - Lakes
HDF-EOS	Hierarchical Data Format - Earth Observing System
HGT	A SRTM file format
HWS	High Water Stage
HYCOS	Hycos Hydraulics & Control Systems
HYPE	Hydrological Predictions for the Environment model
IAG	International Association of Geodesy
IDAN	Intensity-Driven Adaptive-Neighbourhood
IE	Individual Echoes
IGS	International GNSS (Global Navigation Satellite Systems) Service
IM	Internal Meeting (e.g. not with the client)
IODD	Input Output Data Document
IPF	Integrated Processing Facility
ISD	isardSAT
ITRF	International Terrestrial Reference Frame
IRF	Impulse Response Function
Jason-1	Altimetry satellite, T/P follow-on
Jason-2	Altimetry satellite, also knwon as the « Ocean Surface Topography Mission » (OSTM), Jason-1 follow-on
Jason-3	Altimetry satellite, Jason-2 follow-on
Jason-CS	Jason Continuity of Service
KML	Keyhole Markup Language
KO	Kick Off
L1A	Level-1A
L1B	Level-1B
L1B-S, L1BS	Level-1B-S (aka, Stack data)
L2	Level-2
L3	Level-3
L4	Level-4
LAGEOS	Laser Geodynamics Satellite
LEGOS	(french acr.) Laboratoire d'Études en Géophysique et Océanographie Spatiale (Laboratory for Studies in Geophysics and Spatial Oceanography)
LOTUS	Preparing Land and Ocean Take Up from Sentinel-3
LPS	Living Planet Symposium
LRM	Low Resolution Mode
LSE	Least Square Estimator
LWL	Lake Water Level
LWS	Low Water Stage
MARS	Meteorological Archival and Retrieval System
MDL	Minimum Description Length
MMSE	Minimum Mean Square Error
MNDWI	Modification of Normalised Difference Water Index
MoM	Minutes of Meeting
MPC	Mission Performance Centre
MRC	Mekong River Commission
MTR	Mid Term Review
MSS	Mean Square Slope
MSS	Mean Sea Surface
MWR	Microwave Radiometer
NAVATT	Navigation and Attitude
NDVI	Normalised Difference Vegetation Index
NDWI	Normalised Difference Water Index
netCDF	Network Common Data Form
NOAA	National Oceanic and Atmospheric Administration
NR	New Requirement (w.r.t. the SoW)
NRT	Near Real-Time
NWM	Numerical Weather Model
OCOG	Offset Centre of Gravity
OPC	One per Crossing
OSTM	Ocean Surface Topography Mission (also known as Jason-2), is also the name of the satellites series T/P, Jason-1, Jason-2 and Jason-3
OVS	Orbit State Vector
PDF	Probability Density Function
PEACHI	Prototype for Expertise on AltiKa for Coastal, Hydrology and Ice
PEPS	Sentinel Product Exploitation Platform (CNES)
PISTACH	(french acr.) Prototype Innovant de Système de Traitement pour les Applications Cotières et l'Hydrologie
PMP	Project Management Plan
POCCD	Processing Options Configuration Control Document

PR	Progress Report
PRF	Pulse Repetition Frequency
PSD	Product Specification Document
PTR	Point Target Response
PVP	Product Validation Plan
PVR	Product Validation Report
PVS	Pseudo Virtual Station(s)
RADS	Radar Altimeter Database System
RB	Requirements Baseline (document)
RCMC	Range Cell Migration Curve
RCS	Radar Cross Section
RD	Reference Document
RDSAR	Reduced SAR (also known as Pseudo-LRM)
RF	Random Forest
RGB	Red, Green, Blue
RID	Review Item Discrepancy
RIP	Range Integrated Power (of the MLD) sometimes referred as Angular Power Response (APR)
RMS	Root Mean Square
ROI	(geographical) Region(s) Of Interest
RP	Report Period (a month that is being reported into a Progress Report)
RSS	Remote Sensing Systems
RWD	River Water Discharge
RWL	River Water Level
SAMOSA	SAR Altimetry MOde Studies and Applications
SARAL	In Indian "simple", in english "SAtellite for ARgos and AltiKa.
SARIn	SAR Interferometric (CryoSat-2/SIRAL mode)
SAR	Synthetic Aperture Radar
SARvatore	SAR Versatile Altimetric Toolkit for Ocean Research & Exploitation
SCOOP	SAR Altimetry Coastal & Open Ocean Performance
SDP	Software Development Plan
SEOM	Scientific Exploitation of Operational Missions
SHAPE	Sentinel-3 Hydrologic Altimetry PrototypE
SI-MWR	Scanning Imaging MWR
SME	Small and Medium-sized Enterprise
SMHI	Swedish Meteorological and Hydrological Institute
SNAP	SeNtinel Application Platform
SOA	State Of the Art
SOW	Statement Of Work
SPR	Software Problem Reporting
SPS	Sentinel-3 Surface Topography Mission System Performance Simulator
SRAL	SAR Radar Altimeter
SRTM	Shuttle Radar Topography Mission
SSB	Sea State Bias
SSMI/IS	Special Sensor Microwave Imager (SSM/I) Sounder
SSO	Single Sign-On
Stack	Matrix of stacked Doppler beams
STD	Standard Deviation
STM	Sentinel-3 Surface Topography Mission
SUM	Software User Manual
SWBD	SRTM Water Body Data
SWH	Significant Wave Height
TAI	Temps Atomique International (International Atomic Time)
TBC	To Be Confirmed
TBD	To Be Done
TCWV	Total Column Water Vapour
TDS	Test Data Set
TMI	Tropical Rainfall Measuring Mission (TRMM) Microwave Imager
TN	Technical Note
T/P	Topex/Poseidon (altimetry satellite)
TR	Technical Risk
UNESCO	United Nations Educational, Scientific and Cultural Organization
URL	Uniform Resource Locator
USGS	United States Geological Survey
USO	Ultra Stable Oscillator
UTC	Coordinated Universal Time
UWM	Updated Water Mask
VS	Virtual Station(s)
VH	Vertical-Horizontal polarisation
VV	Vertical-Vertical polarisation
WBS	Work Breakdown Structure
WFR	Water Fraction Ratio
WMO	World Meteorological Organization
WP	Work Package(s)
w.r.t.	with respect to
WTC	Wet Tropospheric Correction
XML	eXtensible Markup Language
ZP	Zero Padding